

NPS68 - 82 - 006

# NAVAL POSTGRADUATE SCHOOL

## Monterey, California



Model Simulations of Seventeen Years  
of Mixed Layer Evolution at Ocean Station Papa

Roland W. Garwood

David Adamec

November 1982

Final Report for Period October 1981 - September 1982

Approved for public release; distribution unlimited.

FEDDOCS

D 208.14/2:NPS-68-82-006 Research and Development Activity (Code 320)

Mississippi 39529

NAVAL POSTGRADUATE SCHOOL  
Monterey, California 93940

Rear Admiral J.J. Ekelund  
Superintendent

David A. Schradly  
Provost

The work reported herein is a result of the research project "Modelling Upper Ocean Thermal Structure" supported by the Naval Research and Development Activity, NSTL Station, MS under program element 62759N. Reproduction of all or part of this report is authorized.

This report was prepared by:

SECURITY CLASSIFICATION OF THIS PAGE (When Data Entered)

REPORT DOCUMENTATION PAGE		READ INSTRUCTIONS BEFORE COMPLETING FORM
1. REPORT NUMBER NPS68-82-006	2. GOVT ACCESSION NO.	3. RECIPIENT'S CATALOG NUMBER
4. TITLE (and Subtitle) Model Simulations of Seventenn Years of Mixed Layer Evolution at Ocean Station Papa		5. TYPE OF REPORT & PERIOD COVERED Report for October 1981 - September 1980
		6. PERFORMING ORG. REPORT NUMBER
7. AUTHOR(s) Roland W. Garwood David Adamec		8. CONTRACT OR GRANT NUMBER(s)
9. PERFORMING ORGANIZATION NAME AND ADDRESS Departments of Oceanography and Meteorology Naval Postgraduate School Monterey, California 93940		10. PROGRAM ELEMENT, PROJECT, TASK AREA & WORK UNIT NUMBERS 62759N N6846282WR20098
11. CONTROLLING OFFICE NAME AND ADDRESS Naval Ocean Research & Development Activity NSTL Station, Mississippi 39529		12. REPORT DATE November 1982
		13. NUMBER OF PAGES 37
14. MONITORING AGENCY NAME & ADDRESS (if different from Controlling Office)		15. SECURITY CLASS. (of this report) Unclassified
		15a. DECLASSIFICATION/DOWNGRADING SCHEDULE
16. DISTRIBUTION STATEMENT (of this Report)  Approved for public release; distribution unlimited.		
17. DISTRIBUTION STATEMENT (of the abstract entered in Block 20, if different from Report)		
18. SUPPLEMENTARY NOTES		
19. KEY WORDS (Continue on reverse side if necessary and identify by block number) Ocean thermal prediction Mixed Layer Evolution Atmospheric forcing of the ocean		
20. ABSTRACT (Continue on reverse side if necessary and identify by block number)  The bulk second order closure method of Garwood (1977) is used to predict the well-mixed layer depth and temperature evolution at Ocean Station Papa for the years 1953-1969. The time dependent boundary conditions are the specification of the surface buoyancy flux and wind stress derived from the 3-hourly atmospheric observations. Much of the variance of the well-mixed layer depth and temperature evolution is obviously associated with the annual		

~~UNCLASSIFIED~~

SECURITY CLASSIFICATION OF THIS PAGE(When Data Entered)

cycle. However, a closer inspection of the results reveals a variability related to the synoptic response of the sea-surface temperature and mixed layer depth to both strong and light wind events. The simulations are not intended to be a best fit, but rather a demonstration of the capability of a one-dimensional model to simulate the interannual variability observed at OWS Papa.

~~UNCLASSIFIED~~

SECURITY CLASSIFICATION OF THIS PAGE(When Data Entered)

MODEL SIMULATIONS OF SEVENTEEN YEARS  
OF MIXED LAYER EVOLUTION AT OCEAN STATION PAPA

Roland W. Garwood<sup>1</sup> and David Adamec<sup>2</sup>

Naval Postgraduate School, Monterey, CA 93940 (U.S.A.)

<sup>1</sup>. Department of Oceanography

<sup>2</sup>. Department of Meteorology

## ABSTRACT

The bulk second order closure method of Garwood (1977) is used to predict the well-mixed layer depth and temperature evolution at Ocean Station Papa for the years 1953-1969. The time dependent boundary conditions are the specification of the surface buoyancy flux and wind stress derived from the three-hourly atmospheric observations. Much of the variance of the well-mixed layer depth and temperature evolution is obviously associated with the annual cycle. However, a closer inspection of the results reveals a variability related to the synoptic response of sea-surface temperature and mixed layer depth to both strong and light wind events. The simulations are not intended to be a best fit, but rather a demonstration of the capability of a one-dimensional model to simulate the interannual variability observed at OWS Papa.

## 1. INTRODUCTION

Ocean Station Papa (50N,145W) in the eastern North Pacific Ocean has been the site of a number of one-dimensional model simulations of the oceanic planetary boundary layer or mixed layer. Using the bulk model of Kraus and Turner (1967) at this site, Denman and Miyake (1973) first simulated the mixed layer response to local atmospheric forcing during June 1970 for a twelve-day period. Mellor and Durbin (1975) applied a profile (rather than bulk) turbulence closure model to simulate a few weeks of upper ocean thermal structure evolution for the same time of the year (late spring but after the mixed layer had shallowed). Camp and Elsberry (1978) used three versions of the bulk mixed layer model (Elsberry et al, 1976; Kim, 1976; and Kraus and Turner, 1967) to study periods of fall and early winter deepening in response to strong atmospheric forcing at a number of locations, including Ocean Station Papa. The lengths of these model integrations were up to a month, and a number of different years were examined. The Mixed Layer Experiment (MILE) of August 18 to September 5, 1977 was also situated at Ocean Station Papa. At least two different model simulations have been conducted of the MILE period; Garwood (1978) and Davis et al (1982). All of the above model simulations at Ocean Station Papa were of relatively short duration, and all were during the same half of the year, namely between the months of May and December after the seasonal thermocline had been set up.



For about 30 years, from the early 1950's until 1981, the Canadian Government sponsored a nearly continuous collection of meteorological and oceanographic data at Ocean Station Papa. The Canadian Government has recently terminated ship activities at Papa, thus interrupting one of the few data sets available to oceanographers who wish to study long term variability in the upper ocean. Such observations have included BT drops, air temperature, humidity, wind measurements and sky cover.

The purpose of this study is to report the multi-year evolution of the ocean thermal structure predicted by a boundary layer entrainment model in response to forcing parameters calculated from observations taken at OWS Papa. In spite of the existence of this long time series of observations, until now no model simulations have been reported which are for more than a few weeks in duration, and no study has previously been conducted of the interannual variability in the ocean mixed layer response to the atmosphere. Also, no simulations have previously been conducted for the period of spring transition (usually between March and May at Ocean Station Papa) when the seasonal thermocline is set up. The purpose of this paper is to document the results of a series of seventeen consecutive model integrations (each of one year in duration) that for the first time take full advantage of the continuity of the data set.



## 2. METHOD

The bulk second order closure method of Garwood (1977) is employed as the OPBL model. The required time dependent surface boundary conditions is the specification of the surface buoyancy and momentum flux which are calculated using bulk aerodynamic formulae (Camp and Elsberry, 1978). The forcing is calculated from the observations taken every three hours. Except for the parameterization of the shear production of turbulence, there is no calculation of the momentum budget in this study. For each of the seventeen years, the model is initialized with a mixed layer depth, mixed layer temperature, a temperature jump at the base of the mixed layer and a bottom temperature (in this case 200 m) to which the temperature decreases linearly from that temperature just below the initial mixed layer depth (see Table I for these values). Each of the model runs is also initialized with a salinity profile that is a constant 34 ppt down to the mixed layer depth, decreases linearly to 35 ppt down to a depth of 150 m and remains a constant 35 ppt below 150 m. This salinity profile contributes to the late winter mixed layer, but has no influence upon the evolution of the seasonal thermocline because the surface salinity flux is zero. This is equivalent to precipitation balancing evaporation.

Within the model there are essentially two degrees

of freedom which can be thought of as "tuning parameters". For all seventeen years of integration, only one set of tuning parameters is used. These tuning parameters were calibrated in such a way so that the maximum summer temperature predicted by the model for 1959 is in agreement with the maximum summer temperature observed at OWS Papa during that year. The year 1959 represents no special case but rather a random choice. This was not intended to be a best fit or optimal tuning in this study, but a demonstration of the relative interannual variability that can be simulated by a one dimensional model.

### 3. RESULTS

Each year at OWS Papa is represented by a set of seven figures labeled a-g. Those figures marked 'a' are the observed mixed layer depths from BT drops. The mixed layer depth was defined to be that depth where the water temperature first deviated by .2 C from the surface value. Figures marked 'b' are the model predicted time evolution of water temperature. The mixed layer depth can be inferred from the tight packing of isotherms. Figures marked c-g are a four day running mean of the time series of the observed sea-surface temperature, air temperature, dew point temperature, wind speed and percentage of cloudiness respectively.

For the most part, the seventeen figures are self evident. It is recommended that the reader peruse them

consecutively, looking for interannual differences and similarities. This should be followed by a much closer inspection of each year, with particular attention paid to the synoptic response of sea-surface temperature and mixed layer depth to both strong and light wind events.

Most of the variances in the dew point, sea and air temperatures are obviously associated with the annual cycle. The air (dry bulb) temperature in all of these cases range from winter lows of about 4 C or 5 C to summer highs ranging near the 14 C or 15 C mark. On the average, the wind speeds are higher in the winter than they are in the summer, although the highest values are attained in the late fall. Oddly enough, the percentage of cloudiness is at a minimum when storm activity is at a peak, and maximum cloudiness occurs in the summer.

Since the model predicted values were only saved once a day, the diurnal signal is not evident here, and the annual cycle is the dominant signal. Initially, the mixed layers are deep and the sea-surface temperatures are low. Then, sometime in spring, the upper-ocean winter regime gives way to a summer regime during which the mixed layer is much shallower and the sea-surface temperatures are much higher. As fall approaches and the frequency of storms increase, the mixed layer becomes progressively deeper until once again the winter regime is restored. There is a limit to mixed layer deepening since the dissipation length scale

is limited by the planetary rotation scale ,  $U^*/f$ , where  $U^*$  is the model computed turbulent velocity scale. This prevents the mixed layer from becoming infinitely deep. The halocline prescribed as an initial condition, also may limit deep mixing for some years, as revealed by model integrations having no halocline (not shown here).

Perhaps the most striking feature in the year-to-year variability of the model hindcasts is the way the winter regime is transformed into a summer regime. This phenomenon is sometimes called 'spring transition'. During the spring, the winds are lighter and there is an increase in the net downward heat flux into the mixed layer. The combination of the lack of turbulent kinetic energy to maintain a deep mixed layer and the formation of a layer of buoyant water due to heating, allows a new mixed layer to reform at a shallower depth. In many cases, the transition has an almost sudden occurrence as is the case for 1959 (Fig. 7a), while with other cases, the change from a winter to a summer regime is more gradual and occurs in two or more steps as in 1957 (Fig. 5a). As suggested by Elsberry and Garwood (1978), the date of spring transition strongly influences summertime sea-surface temperatures. An early transition means that heat accumulates in a shallower boundary layer for a long period of time and hence increases summer sea-surface temperatures more than usual. Conversely, a late transition date will lead to relatively cooler summer temperatures. At OWS Papa, spring transition normally occurs

between Julian days 100 and 120.

In conclusion, the bulk method used here seems to be capable of simulating the seasonal and synoptic-scale variability observed at OWS Papa. Seventeen years of air-sea observations and model integrations provide an extensive test. Certainly other effects such as advection would be needed to provide a complete explanation of ocean variability at OWS Papa, but it is nevertheless encouraging that one dimensional mixing can account for a large part of the variance on time scales from the synoptic to more than a year.

## ACKNOWLEDGMENTS

The authors thank their colleagues Russ Elsberry and Bob Haney for their helpful suggestions in the preparation of this manuscript. This research was funded by the Naval Ocean Research Activity, NSTL Station, Mississippi under contract N684628WR20098. Computer time was supplied by the W.R. Church Computer Center at the Naval Postgraduate School.



## REFERENCES

- Camp, N.T., and R.L. Elsberry, Oceanic thermal response to strong atmospheric forcing, 2, The role of one dimensional processes, 'J. Phys. Oceanogr.', 8, 215-224, 1978.
- Davis, R.E., R. DeSzoeko and P.P. Niiler, Variability in the upper ocean during MILE, 2, Modeling the mixed layer response, 'Deep Sea Research', 28, 1453-1476, 1982.
- Denman, K.I. and M. Miyake, Upper layer modification at ocean station Papa: Observations and simulation. 'J. Phys. Oceanogr.', 3, 185-196, 1973.
- Elsberry, R.L., T. Fraim, and R. Trapnell Jr., A mixed layer model of the oceanic thermal response to hurricanes, 'J. Geophys. Res.', 81, 1153-1162, 1976.
- Elsberry, R.L. and R.W. Garwood Jr., Sea-surface temperature anomaly generation in relation to atmospheric storms, 'Bull. Am. Meteorol. Soc.', 59, 786-789, 1978.
- Garwood, R.W., Jr., An oceanic mixed layer model capable of simulating cyclic states, 'J. Phys. Oceanogr.', 7, 455-468, 1977.
- Garwood, R.W., Evidence of planetary-scale dissipation in the summertime oceanic boundary layer, 'Trans. Am. Geophys. Union', 58, 1156, 1978.
- Kim, J.W., A generalized bulk method of the oceanic mixed layer, 'J. Phys. Oceanogr.', 6, 686-695, 1976.
- Kraus, E.B. and J.S. Turner, A one dimensional model of the seasonal thermocline, 2, The general theory and its consequences, 'Tellus', 19, 98-106, 1967.
- Mellor, G.L. and P.A. Durbin, The structure and dynamics of the ocean surface mixed layer, 'J. Phys. Oceanogr.', 5, 718-728, 1975.

## TABLE AND FIGURE CAPTIONS

Table I Listing of initial sea-surface temperature, mixed layer depth, temperature jump at the base of the mixed layer and temperature at 200 meters for the years 1953-1969.

Fig. 1. (a) Mixed Layer depths from BT drops, (b) depth vs. time contours of temperature, (c) sea-surface temperature, (d) air temperature (e) dew point temperature, (f) wind speed and (g) cloud cover for year 1953.

Fig. 2. As in Figure 1 but for 1954.

Fig. 3. As in Figure 1 but for 1955.

Fig. 4. As in Figure 1 but for 1956.

Fig. 5. As in Figure 1 but for 1957.

Fig. 6. As in Figure 1 but for 1958.

Fig. 7. As in Figure 1 but for 1959.

Fig. 8. As in Figure 1 but for 1960.

Fig. 9. As in Figure 1 but for 1961.

Fig. 10. As in Figure 1 but for 1962.

Fig. 11. As in Figure 1 but for 1963.

Fig. 12. As in Figure 1 but for 1964.

Fig. 13. As in Figure 1 but for 1965.

Fig. 14. As in Figure 1 but for 1966.

Fig. 15. As in Figure 1 but for 1967.

Fig. 16. As in Figure 1 but for 1968.

Fig. 17. As in Figure 1 but for 1969.

# Table I

	Depth	Temp.	T jmp	T bot
1953	100.0	5.6	0.9	3.4
1954	120.0	5.4	0.7	3.4
1955	115.0	5.9	1.2	3.4
1956	120.0	5.5	1.4	3.0
1957	100.0	5.7	0.9	3.4
1958	120.0	7.0	0.9	3.2
1959	105.0	6.0	0.6	4.0
1960	110.0	6.5	1.5	4.0
1961	110.0	5.7	0.7	4.3
1962	100.0	6.0	1.5	3.8
1963	125.0	6.3	1.3	4.0
1964	100.0	5.7	1.3	2.8
1965	120.0	5.0	0.6	2.8
1966	130.0	5.9	1.0	3.6
1967	120.0	6.6	1.4	3.2
1968	130.0	5.3	0.5	3.2
1969	110.0	5.6	0.8	3.2

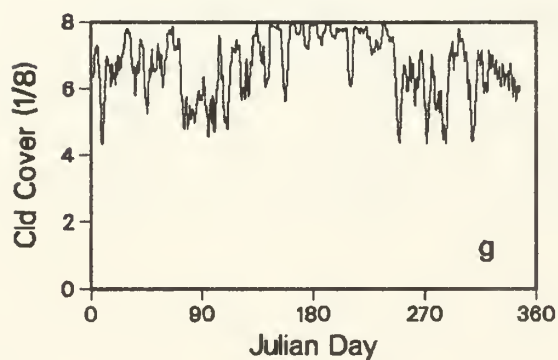
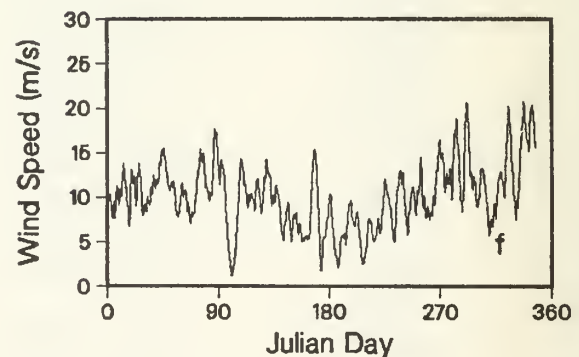
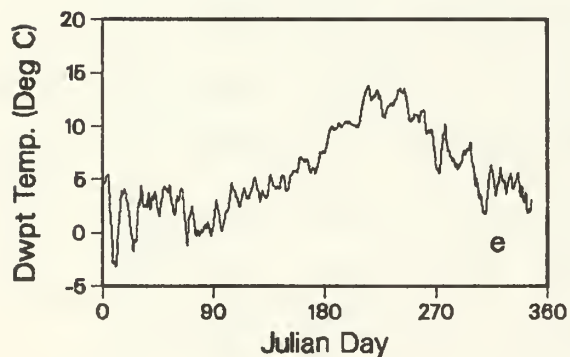
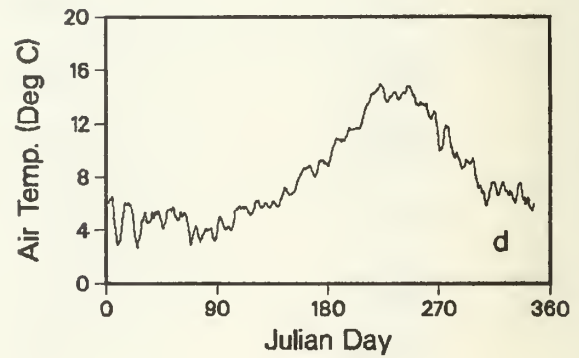
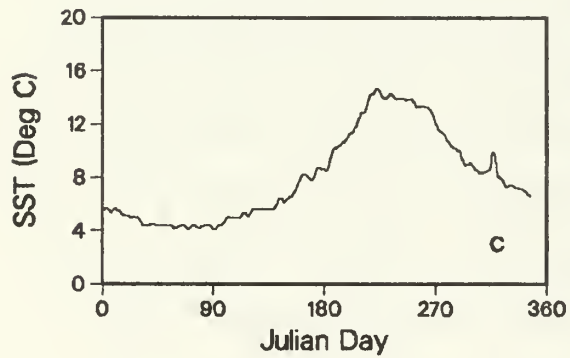
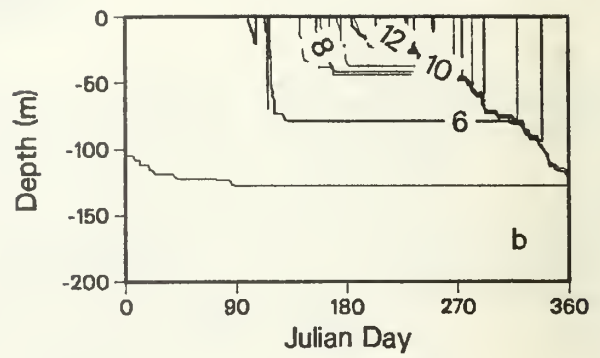
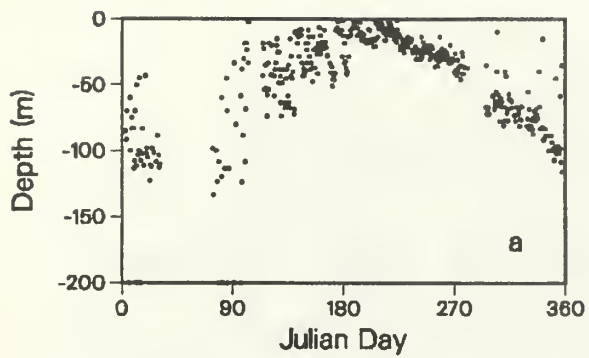


Figure 1. (a) Mixed layer depths from BT drops, (b) depth vs. time contours of temperature, (c) sea-surface temperature, (d) air temperature, (e) dew point temperature, (f) wind speed and (g) cloud cover for year 1953.

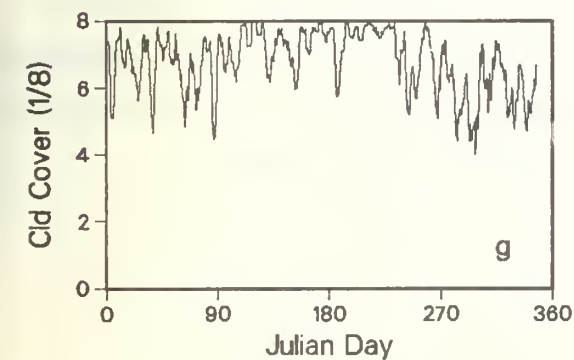
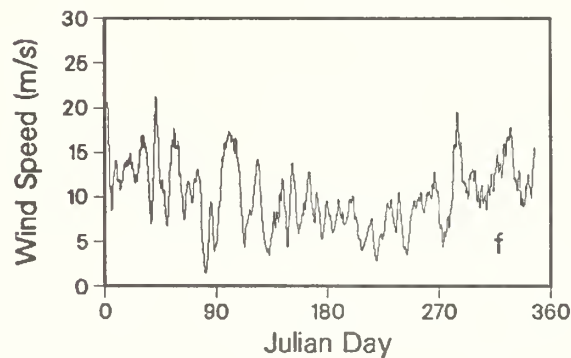
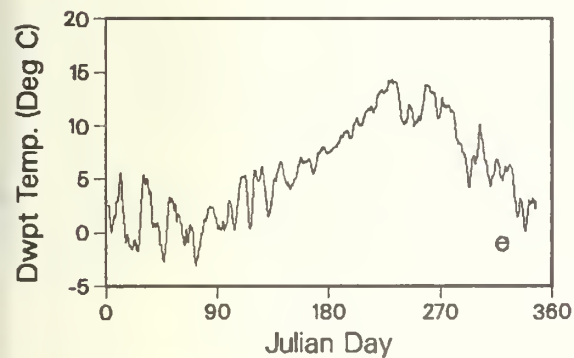
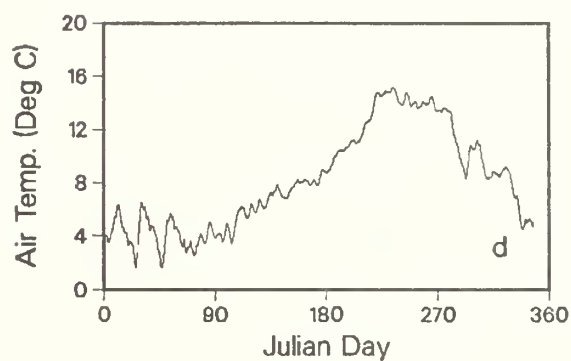
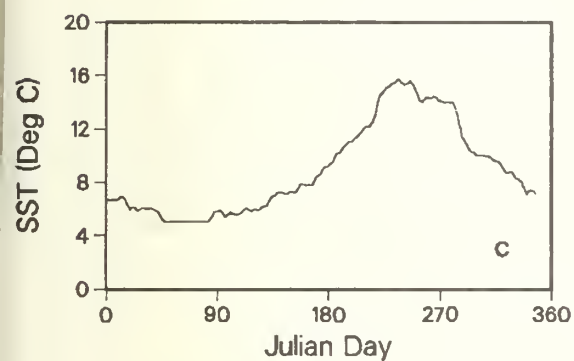
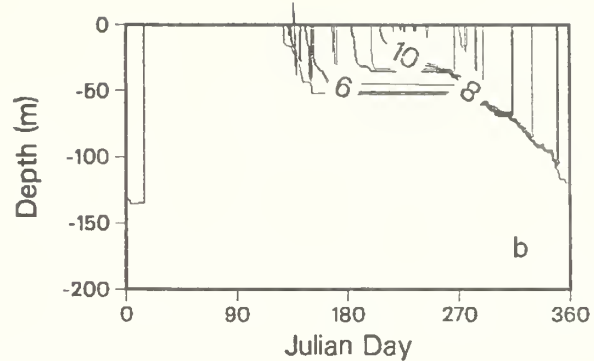
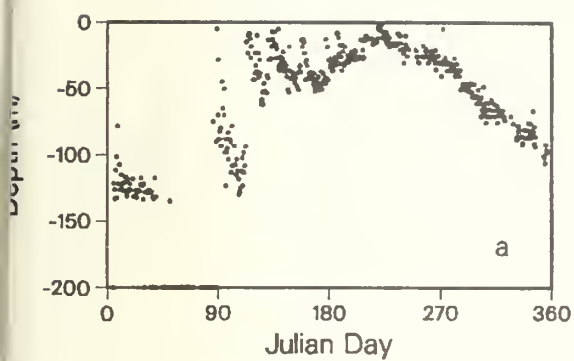


Figure 2. (a) Mixed layer depths from BT drops, (b) depth vs. time contours of temperature, (c) sea-surface temperature, (d) air temperature, (e) dew point temperature, (f) wind speed and (g) cloud cover for year 1954.

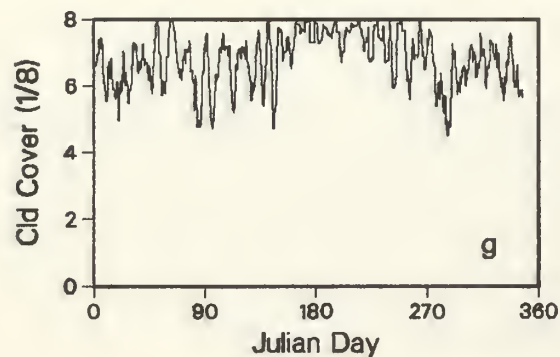
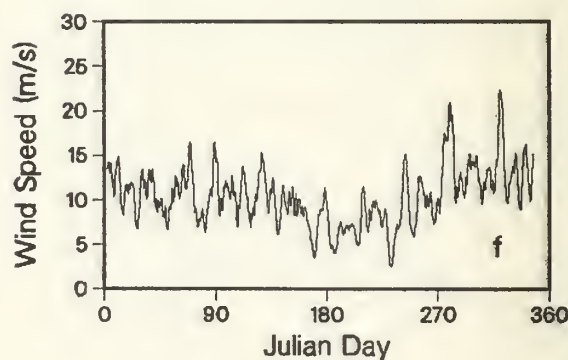
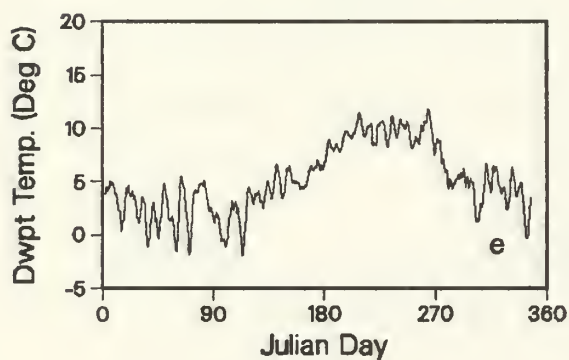
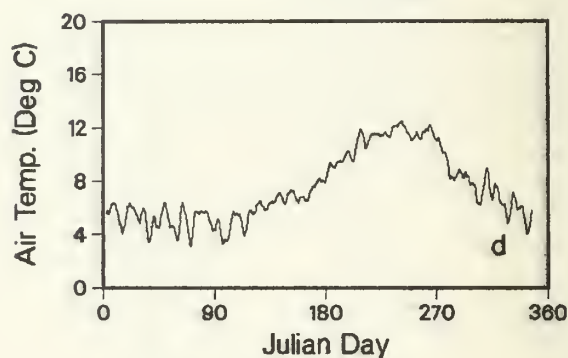
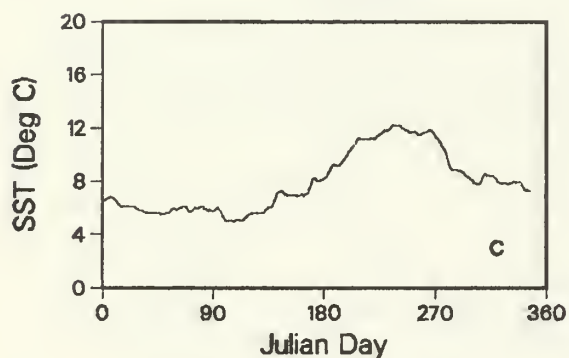
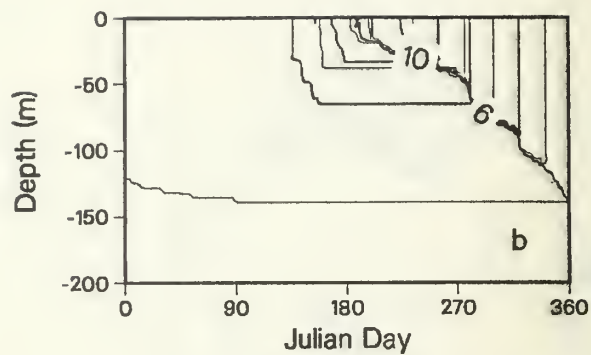
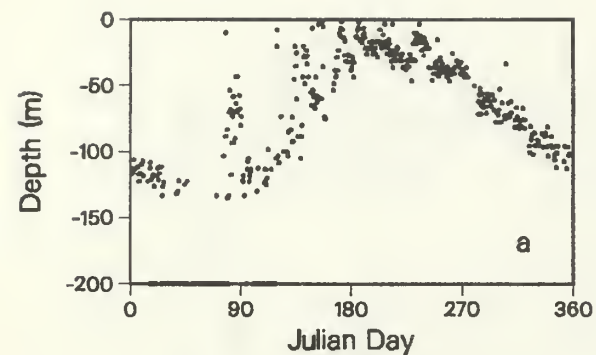


Figure 3. (a) Mixed layer depths from BT drops, (b) depth vs. time contours of temperature, (c) sea-surface temperature, (d) air temperature, (e) dew point temperature, (f) wind speed and (g) cloud cover for year 1955.



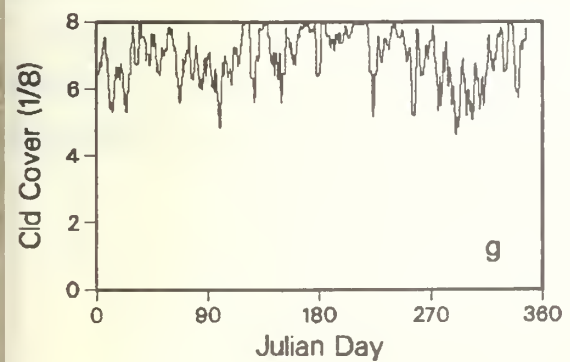
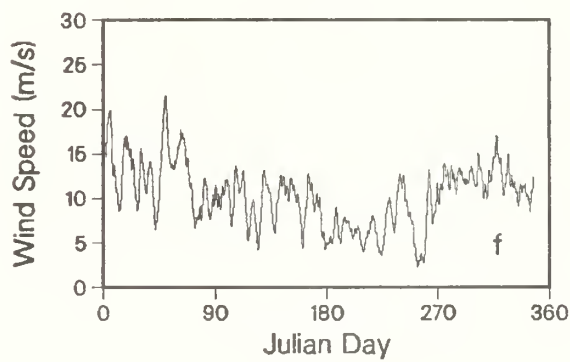
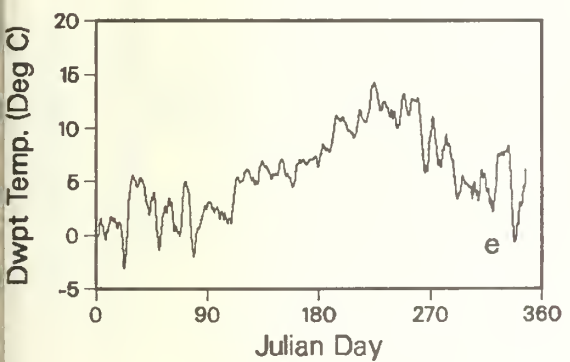
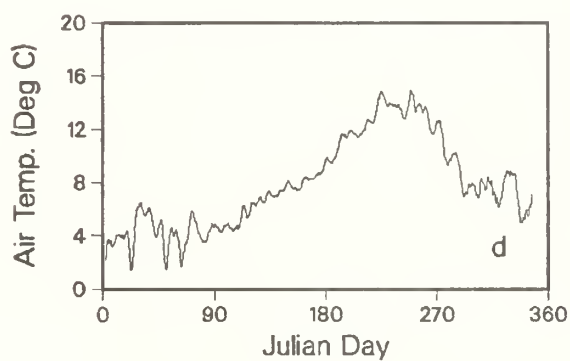
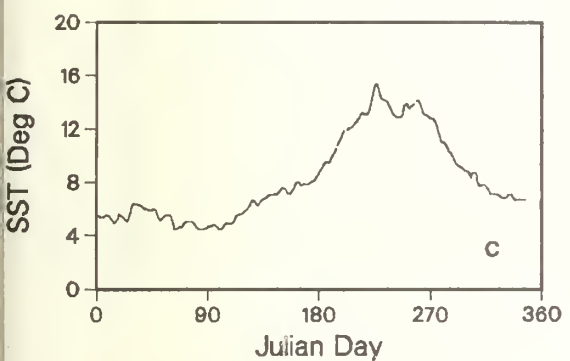
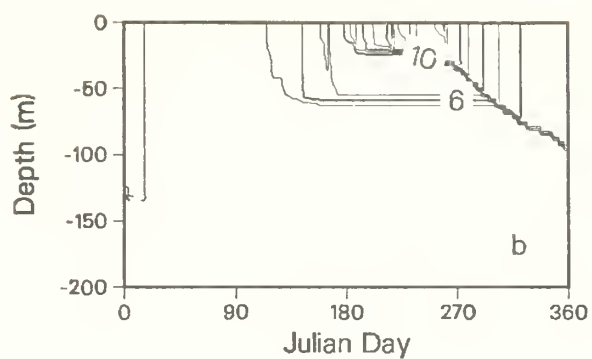
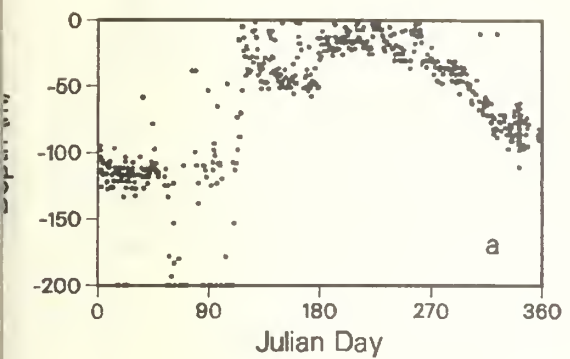


Figure 4. (a) Mixed layer depths from BT drops, (b) depth vs. time contours of temperature, (c) sea-surface temperature, (d) air temperature, (e) dew point temperature, (f) wind speed and (g) cloud cover for year 1956.

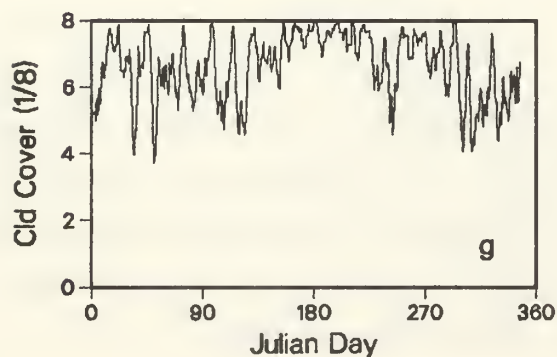
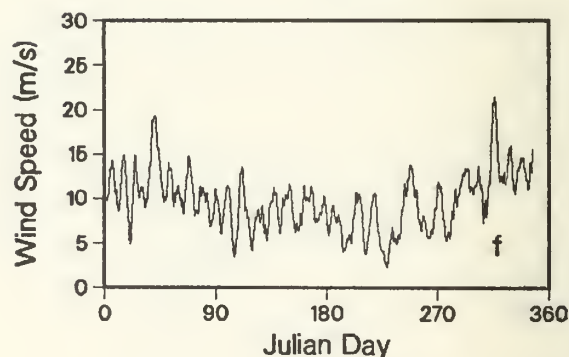
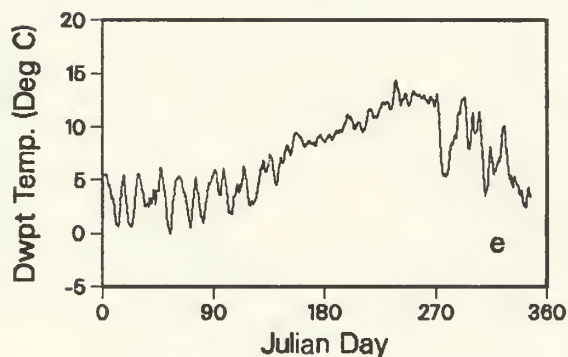
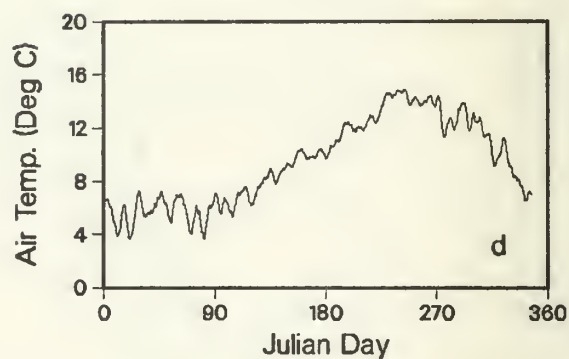
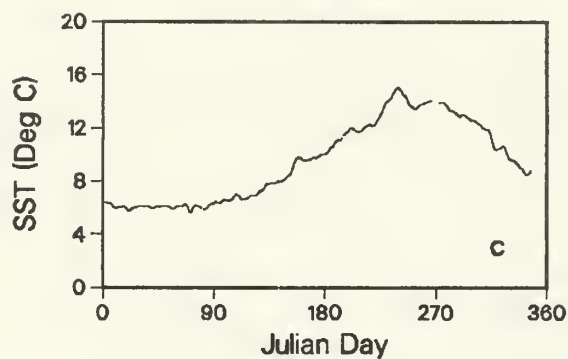
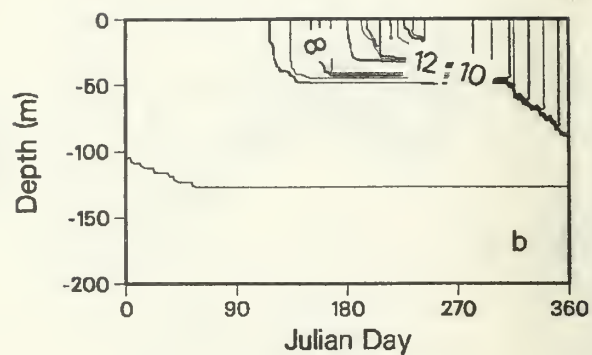
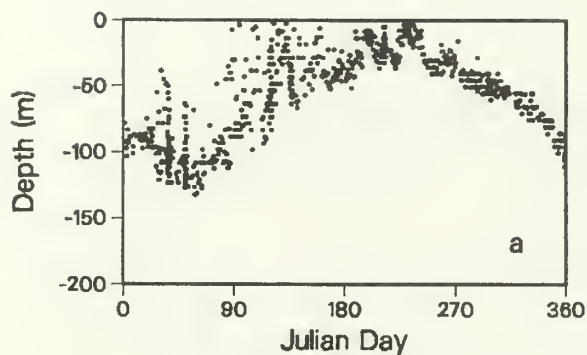


Figure 5. (a) Mixed layer depths from BT drop (b) depth vs. time contours of temperature, (c) sea-surface temperature, (d) air temperature (e) dew point temperature, (f) wind speed and (g) cloud cover for year 1957.

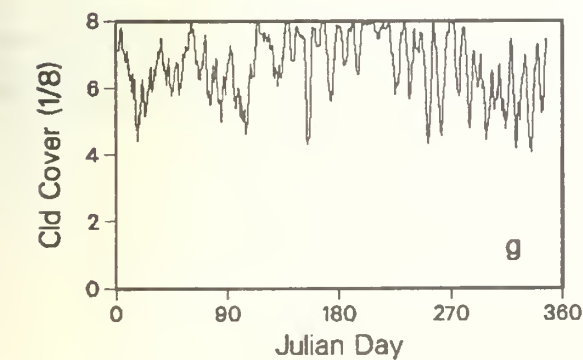
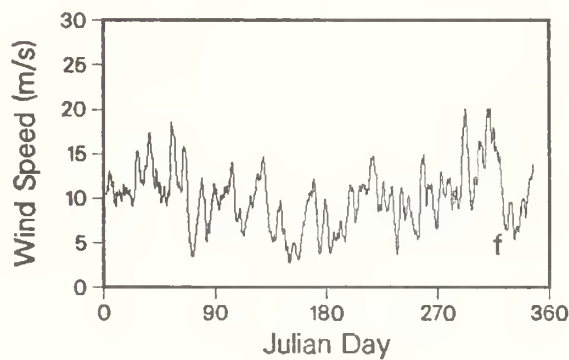
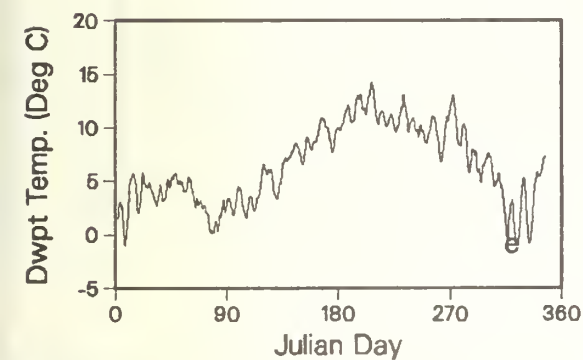
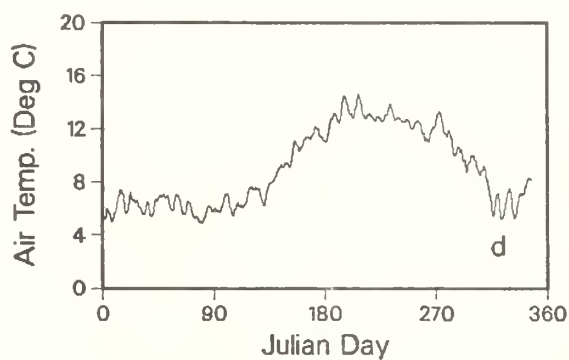
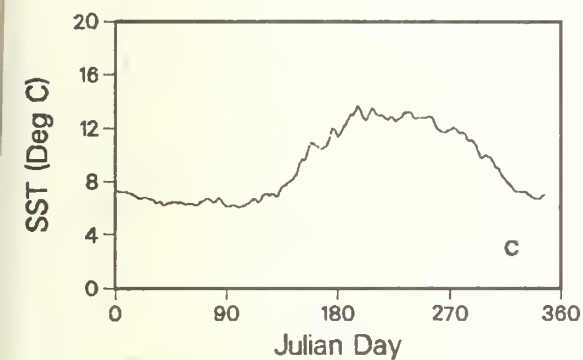
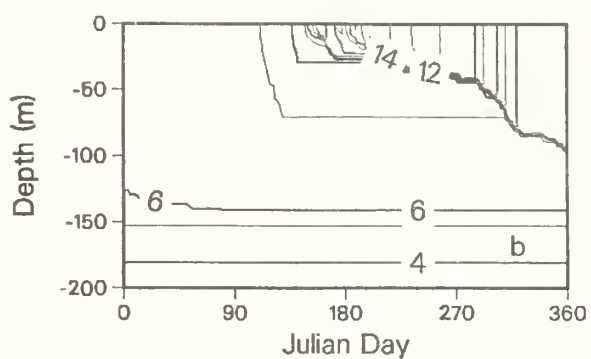
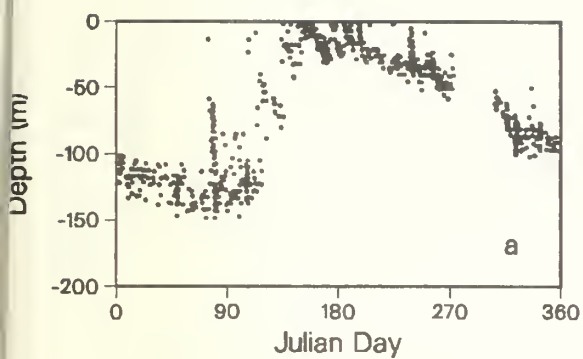


Figure 6. (a) Mixed layer depths from BT drops, (b) depth vs. time contours of temperature, (c) sea-surface temperature, (d) air temperature, (e) dew point temperature, (f) wind speed and (g) cloud cover for year 1958.

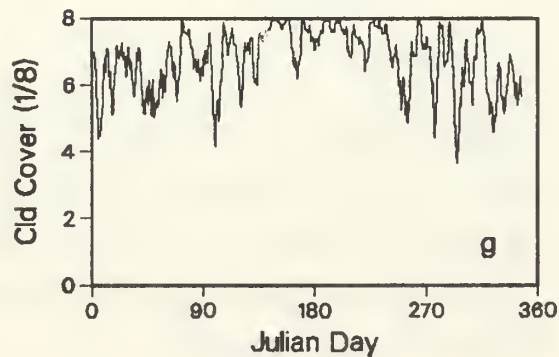
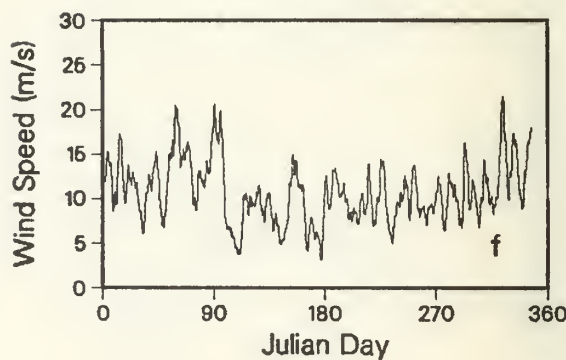
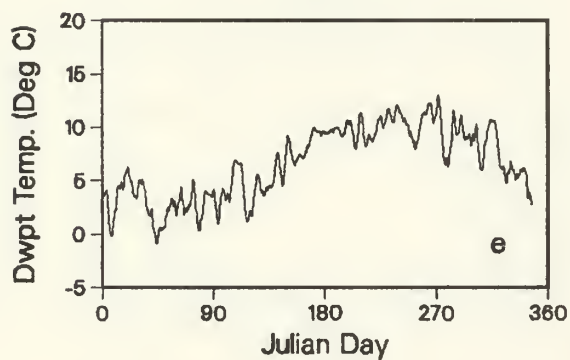
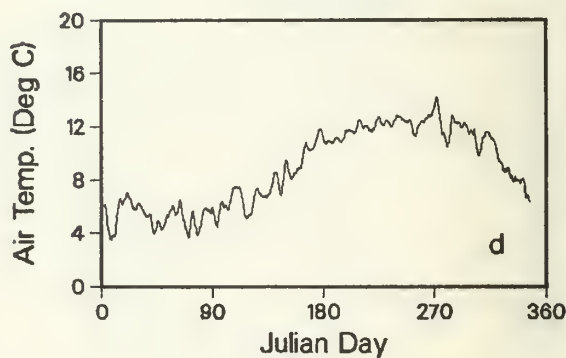
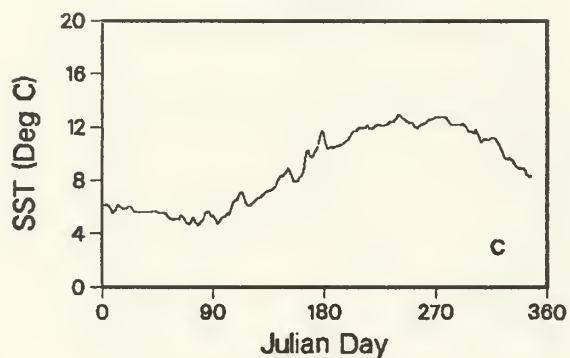
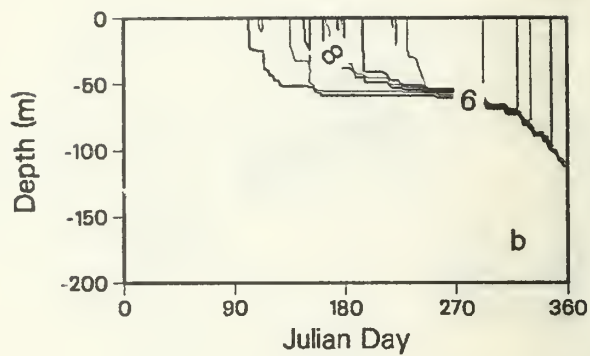
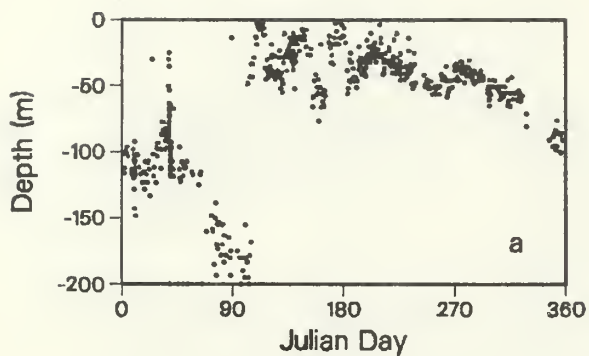


Figure 7. (a) Mixed layer depths from BT drops, (b) depth vs. time contours of temperature, (c) sea-surface temperature, (d) air temperature, (e) dew point temperature, (f) wind speed and (g) cloud cover for year 1959.

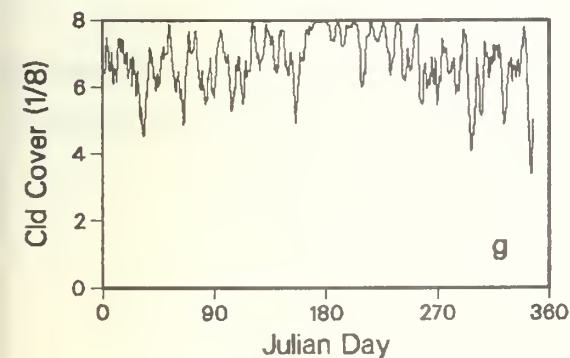
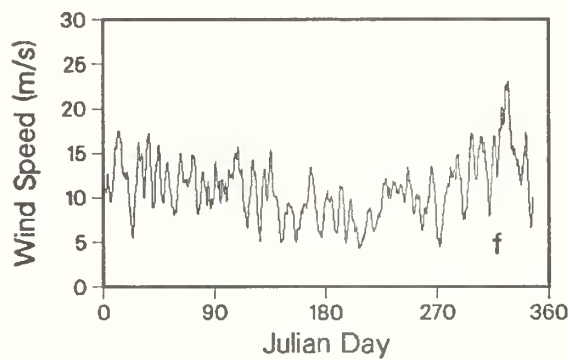
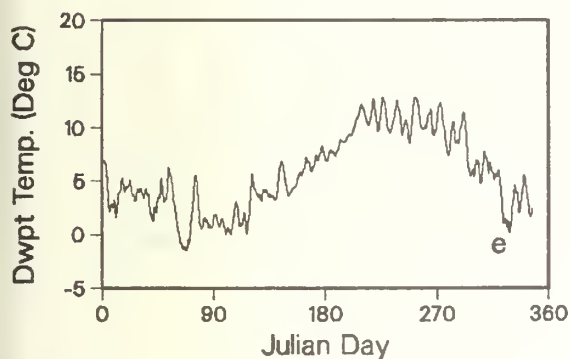
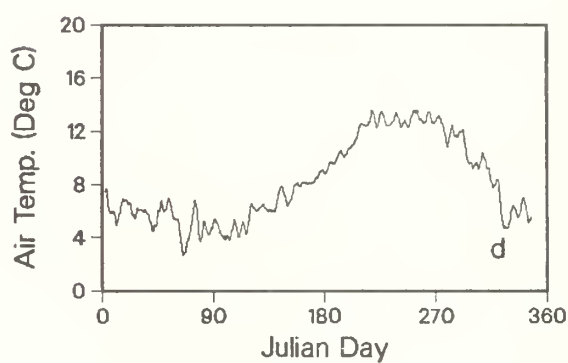
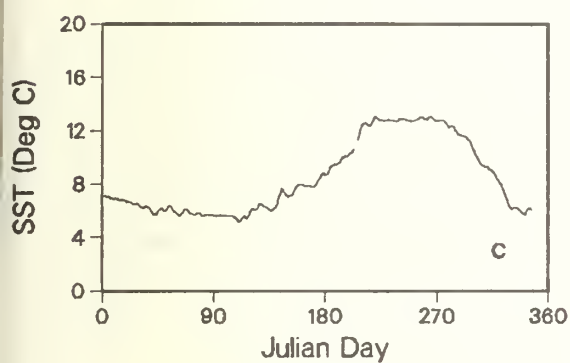
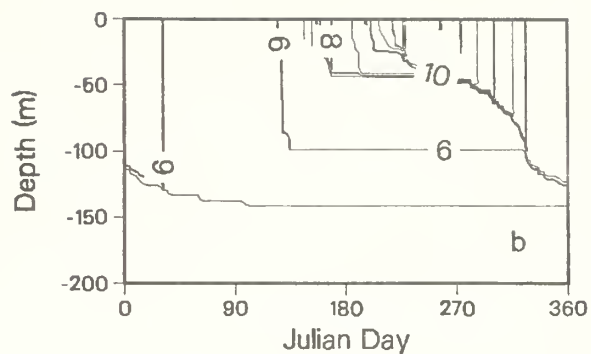
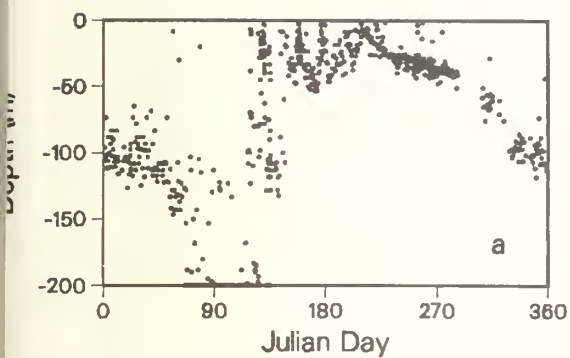


Figure 8. (a) Mixed layer depths from BT drops, (b) depth vs. time contours of temperature, (c) sea-surface temperature, (d) air temperature, (e) dew point temperature, (f) wind speed and (g) cloud cover for year 1960.



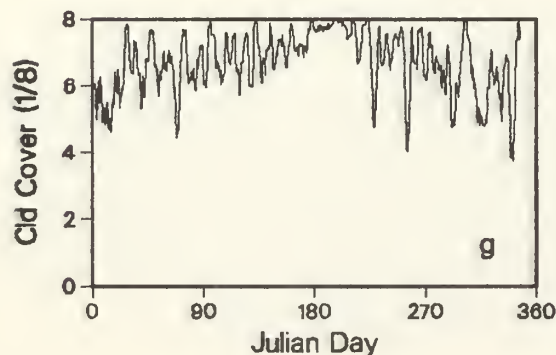
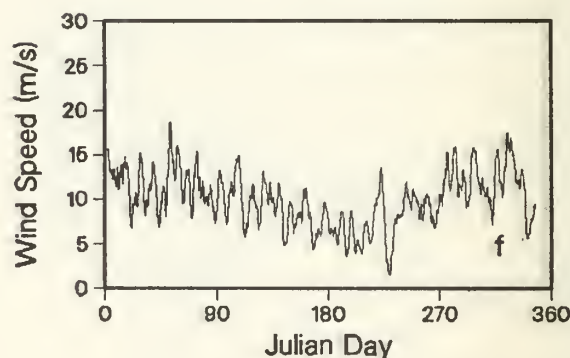
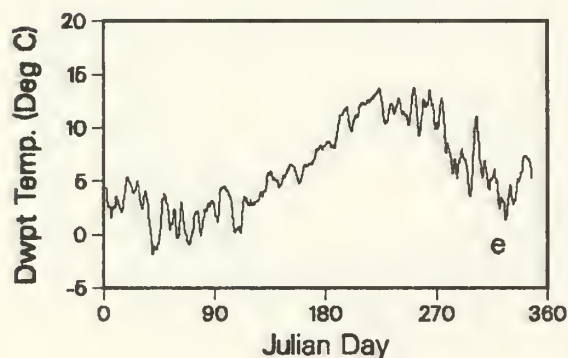
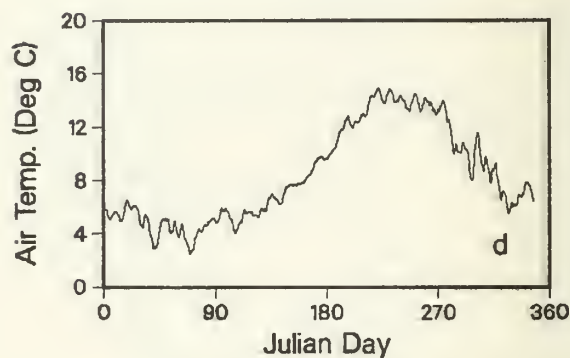
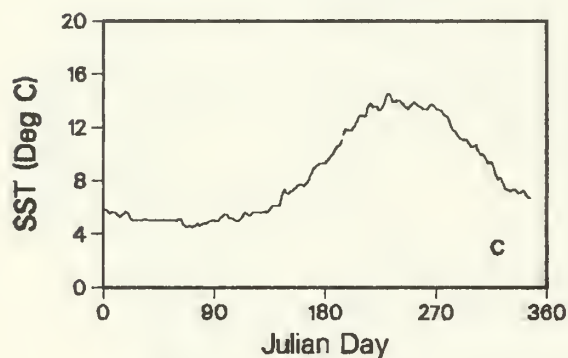
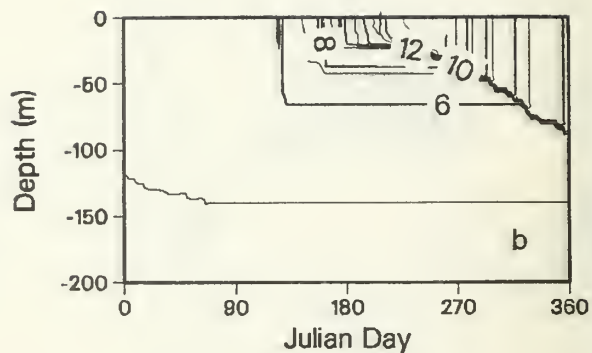
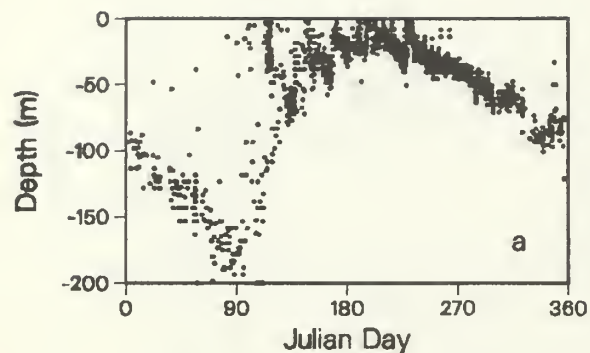


Figure 9. (a) Mixed layer depths from BT drops, (b) depth vs. time contours of temperature, (c) sea-surface temperature, (d) air temperature, (e) dew point temperature, (f) wind speed and (g) cloud cover for year 1961.



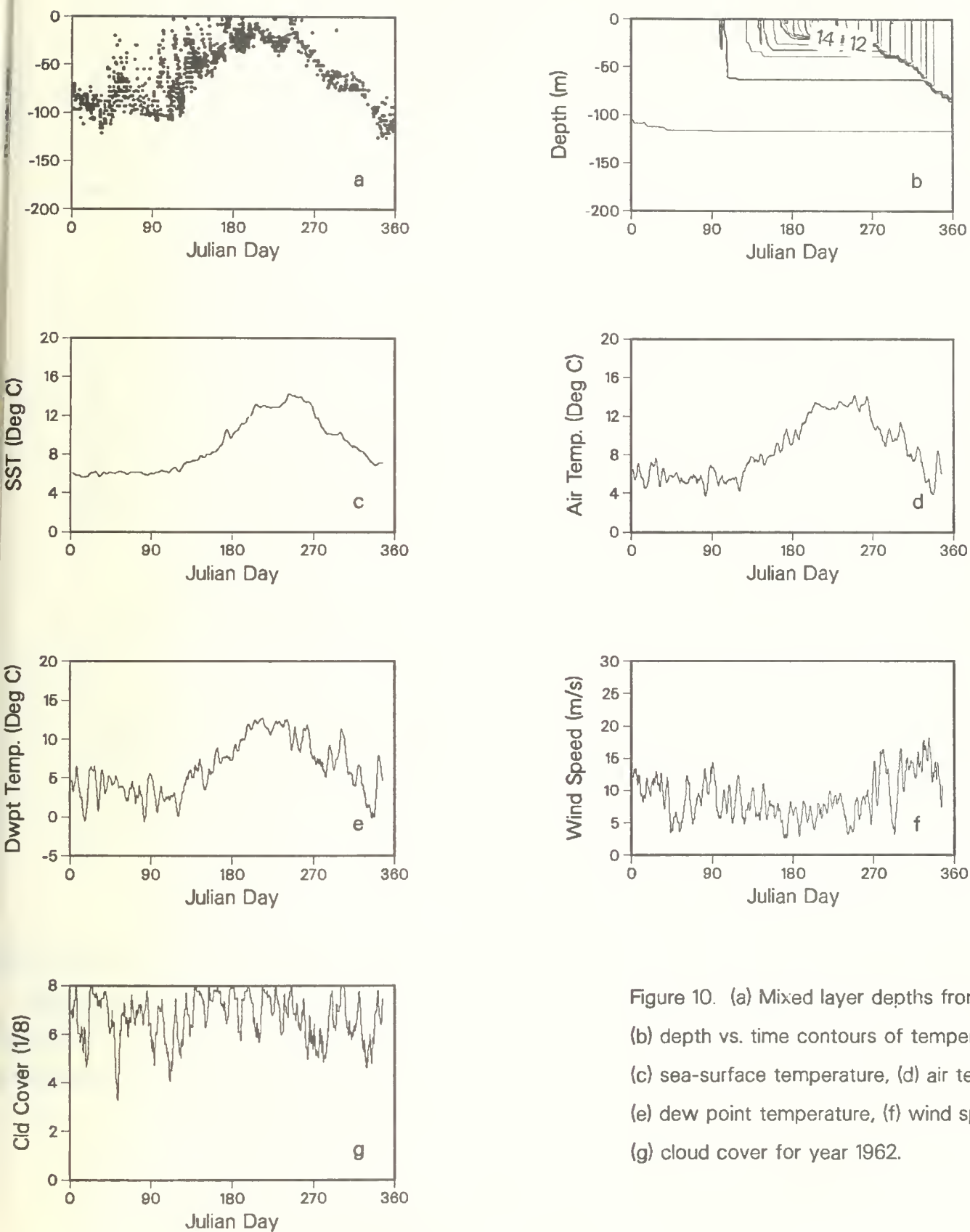


Figure 10. (a) Mixed layer depths from BT drops, (b) depth vs. time contours of temperature, (c) sea-surface temperature, (d) air temperature, (e) dew point temperature, (f) wind speed and (g) cloud cover for year 1962.

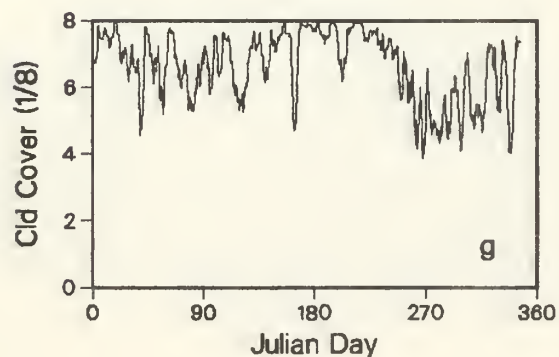
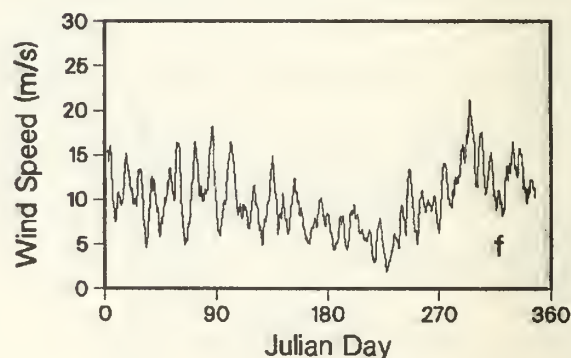
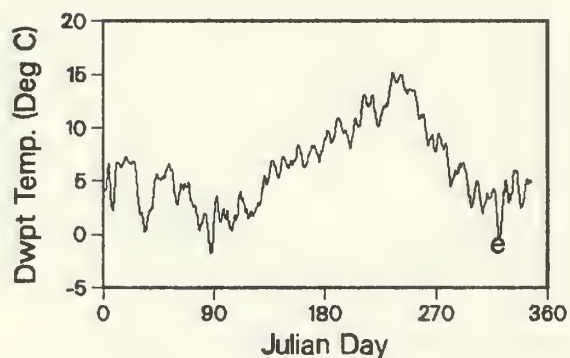
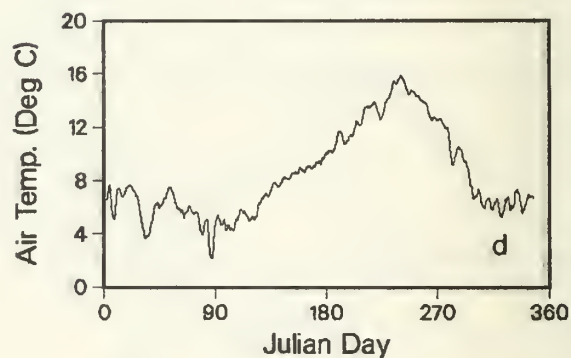
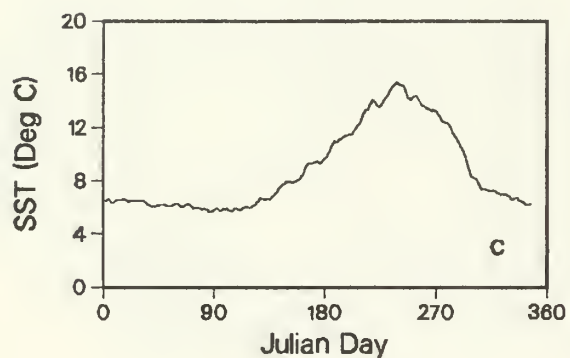
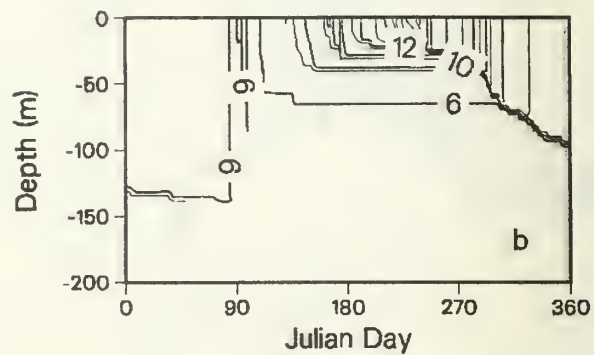
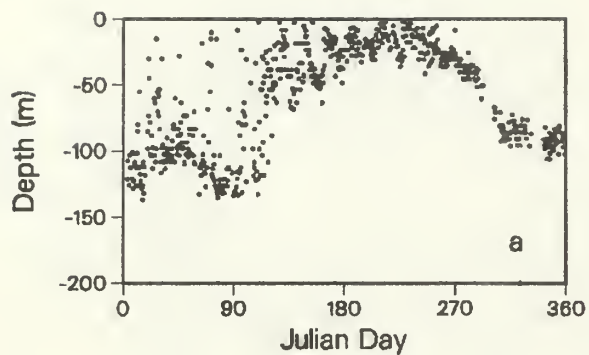


Figure 11. (a) Mixed layer depths from BT drop (b) depth vs. time contours of temperature, (c) sea-surface temperature, (d) air temperature (e) dew point temperature, (f) wind speed and (g) cloud cover for year 1963.

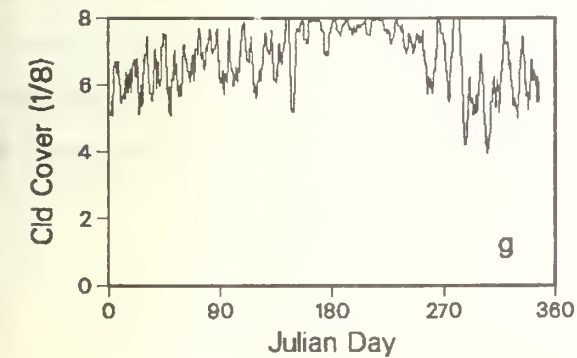
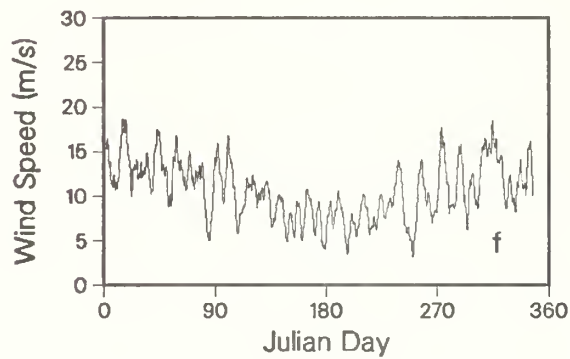
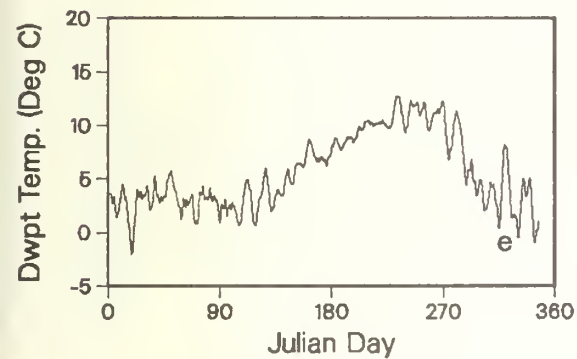
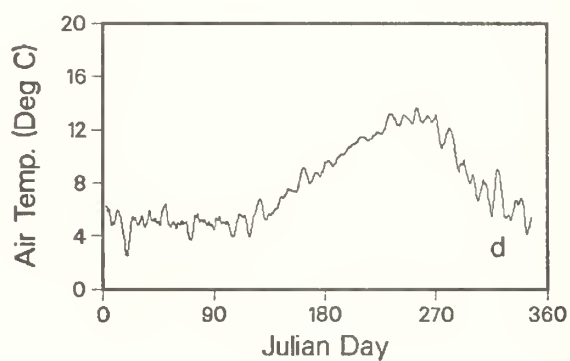
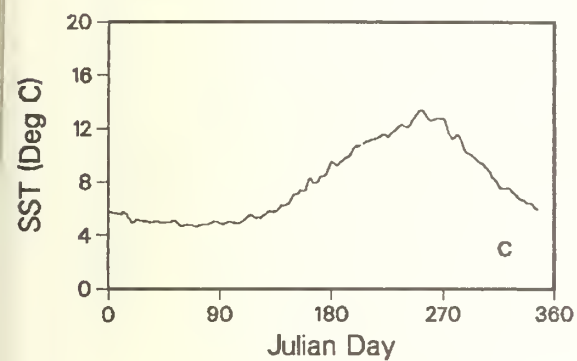
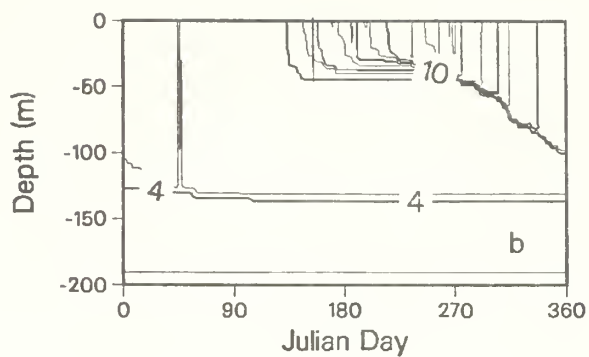
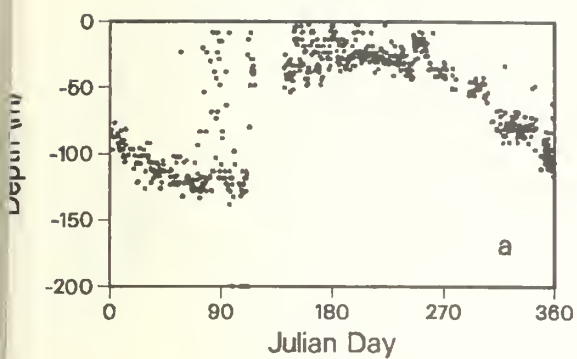


Figure 12. (a) Mixed layer depths from BT drops, (b) depth vs. time contours of temperature, (c) sea-surface temperature, (d) air temperature, (e) dew point temperature, (f) wind speed and (g) cloud cover for year 1964.

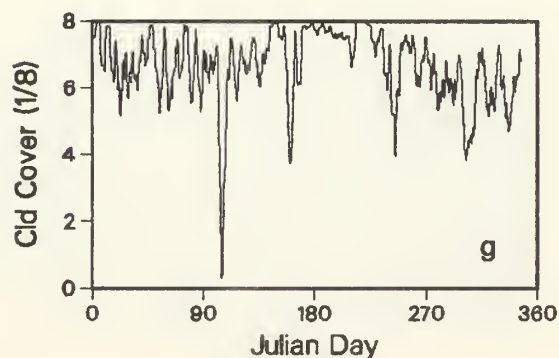
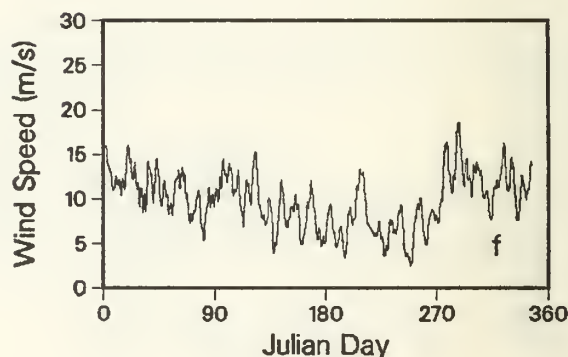
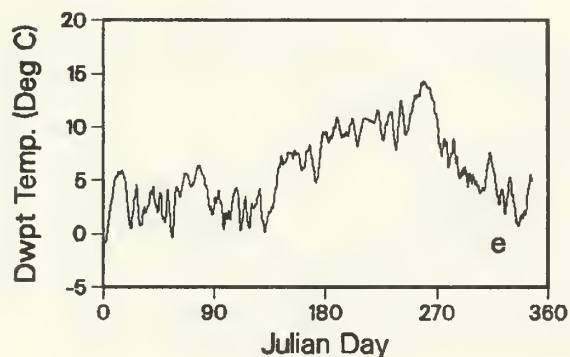
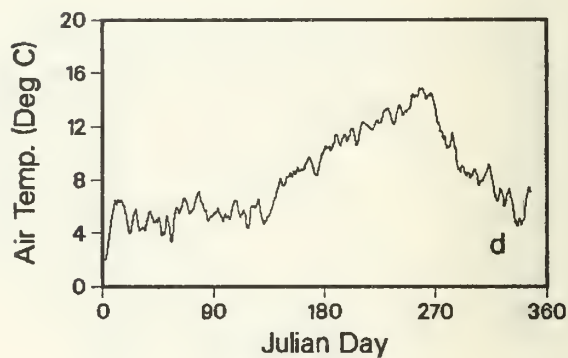
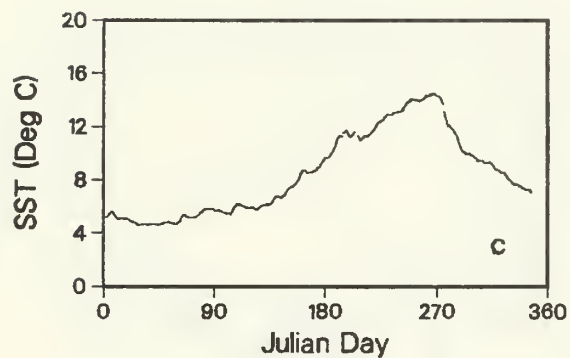
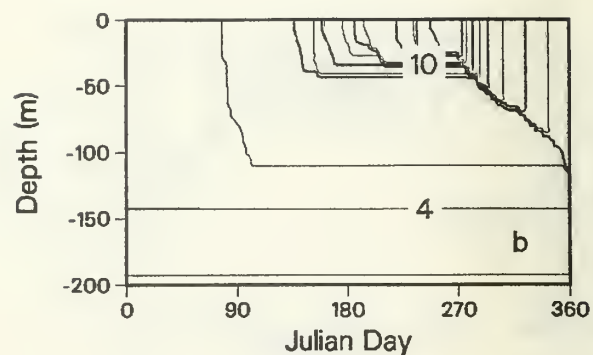
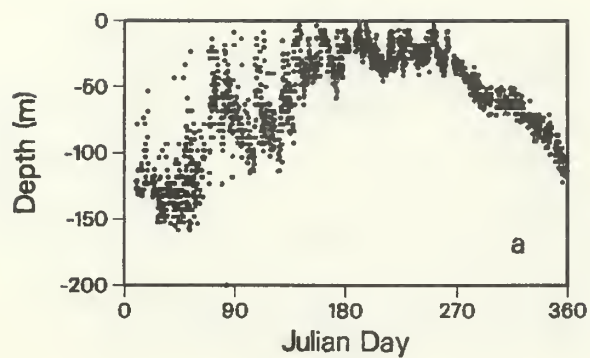


Figure 13. (a) Mixed layer depths from BT dr. (b) depth vs. time contours of temperature, (c) sea-surface temperature, (d) air temperature, (e) dew point temperature, (f) wind speed and (g) cloud cover for year 1965.

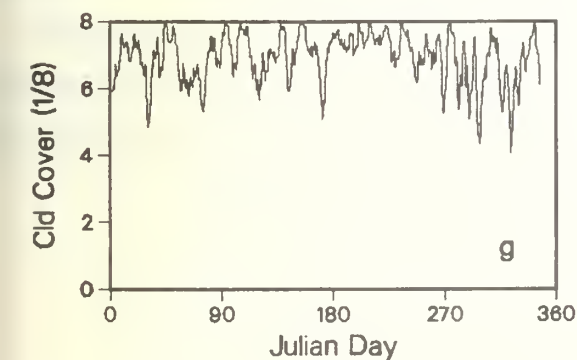
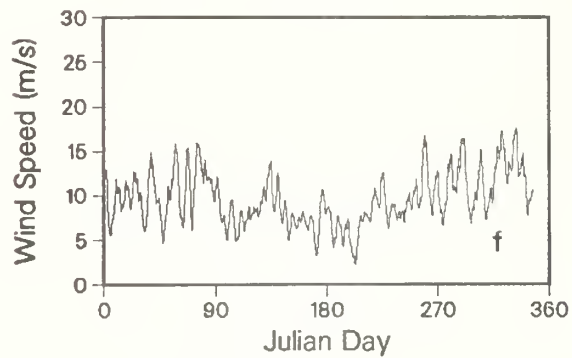
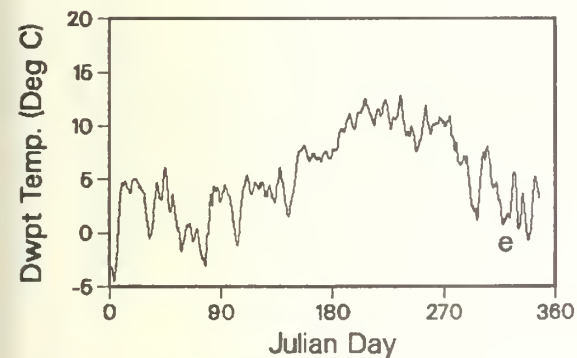
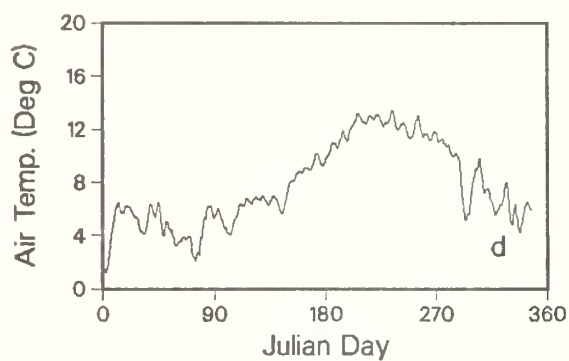
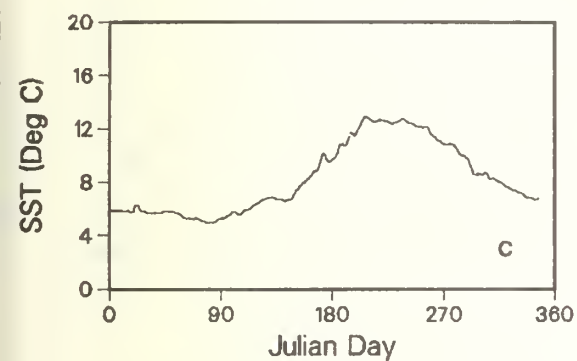
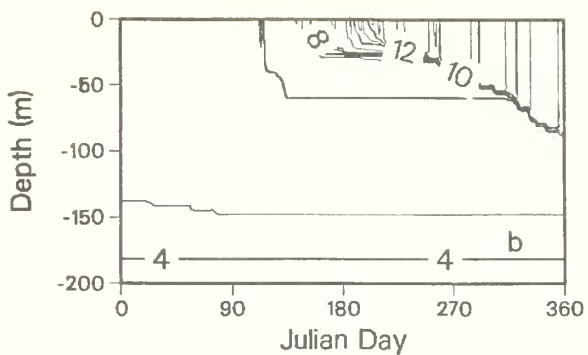
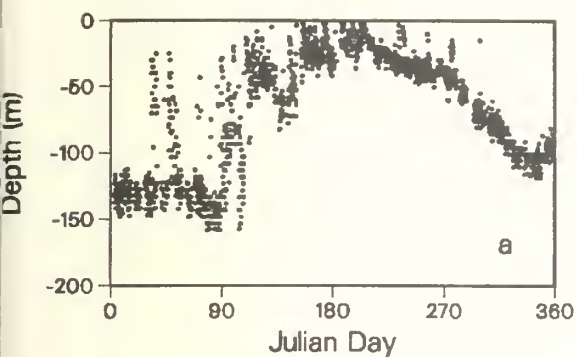


Figure 14. (a) Mixed layer depths from BT drops, (b) depth vs. time contours of temperature, (c) sea-surface temperature, (d) air temperature, (e) dew point temperature, (f) wind speed and (g) cloud cover for year 1966.



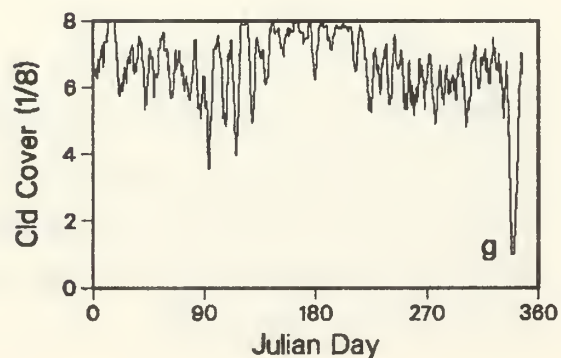
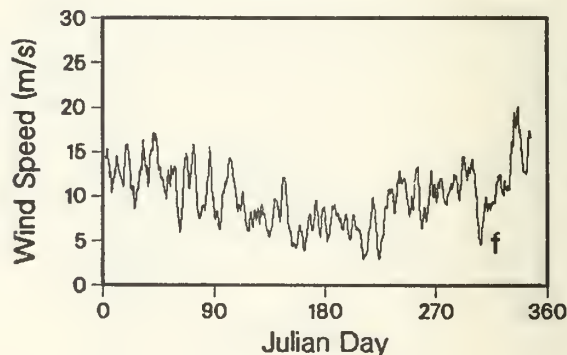
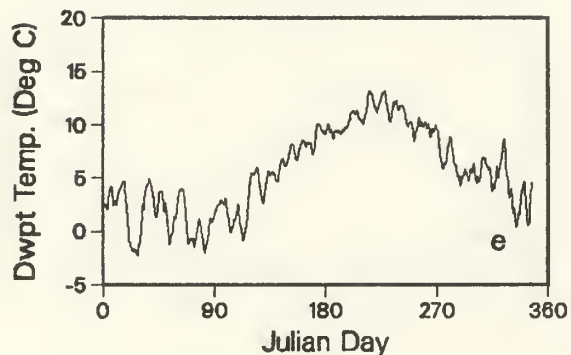
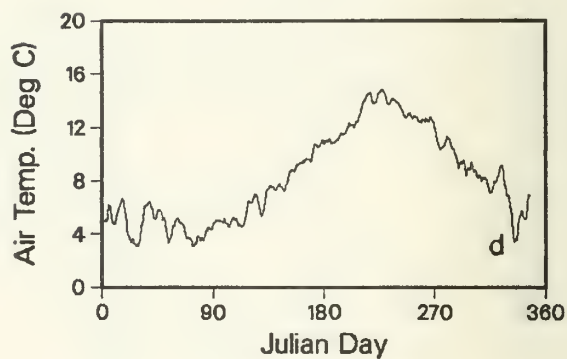
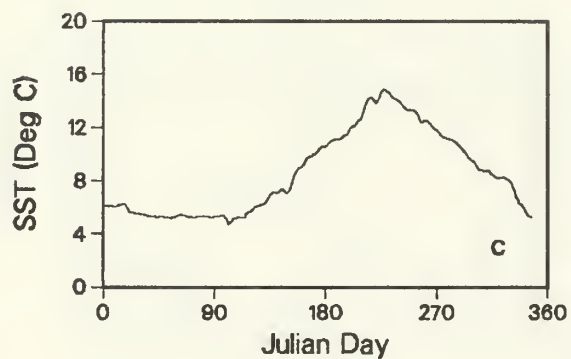
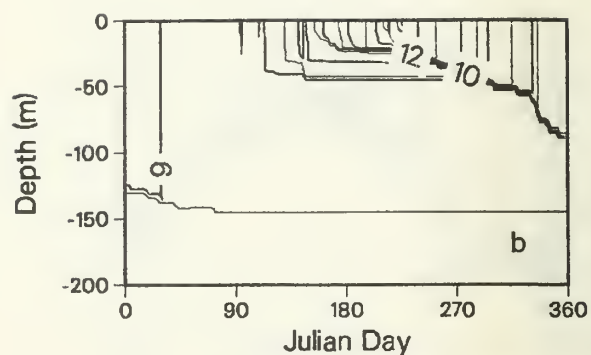
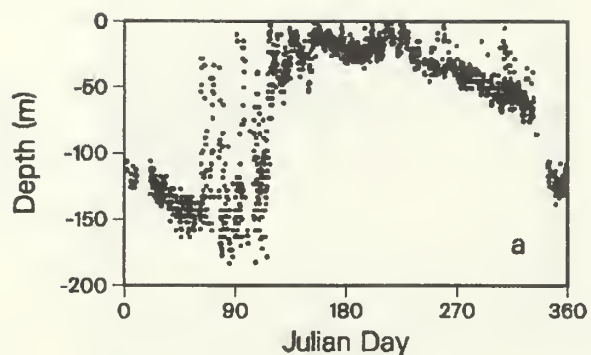


Figure 15. (a) Mixed layer depths from BT data, (b) depth vs. time contours of temperature, (c) sea-surface temperature, (d) air temperature, (e) dew point temperature, (f) wind speed and (g) cloud cover for year 1967.



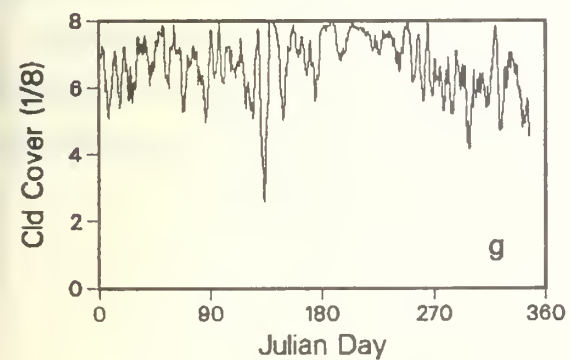
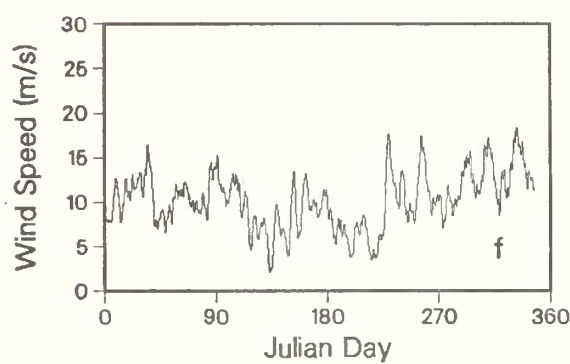
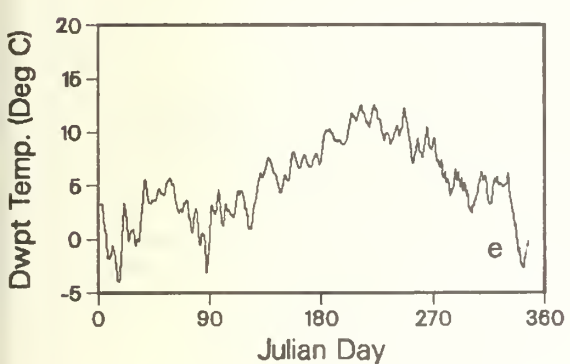
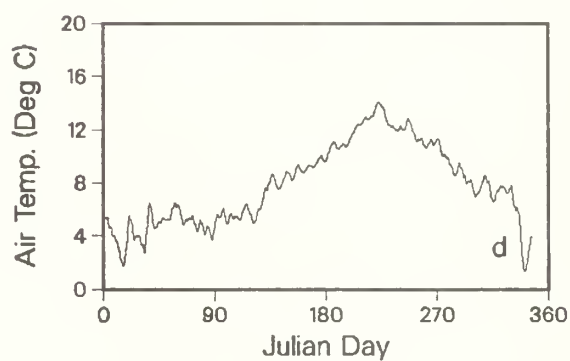
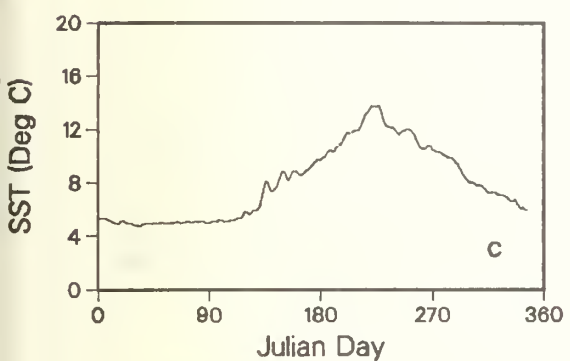
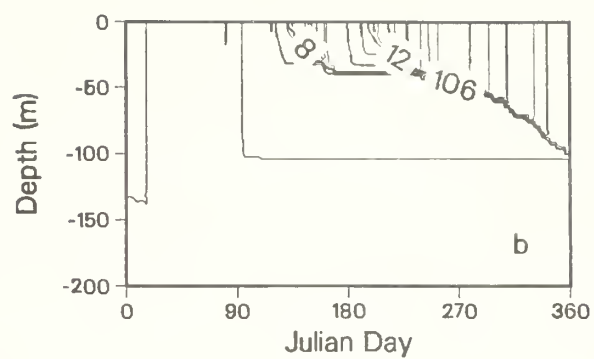
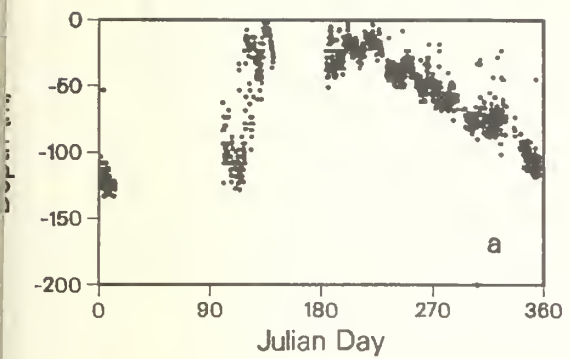


Figure 16. (a) Mixed layer depths from BT drops, (b) depth vs. time contours of temperature, (c) sea-surface temperature, (d) air temperature, (e) dew point temperature, (f) wind speed and (g) cloud cover for year 1968.

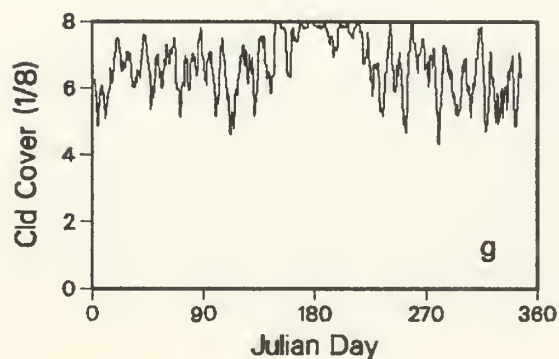
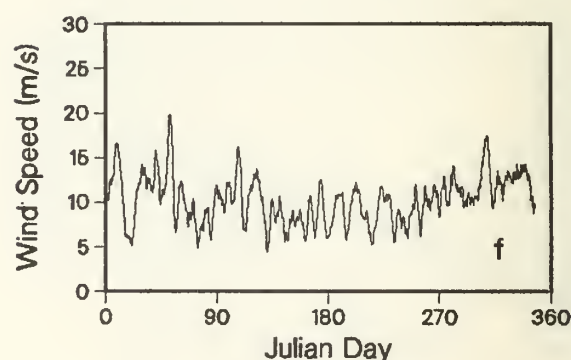
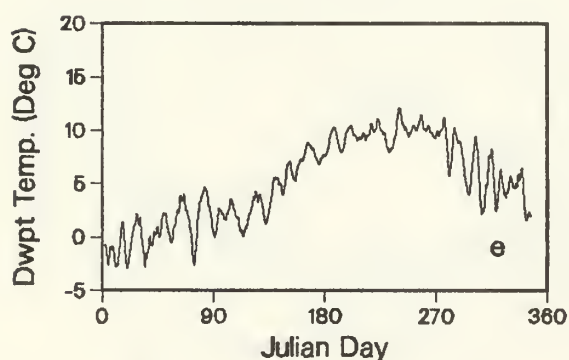
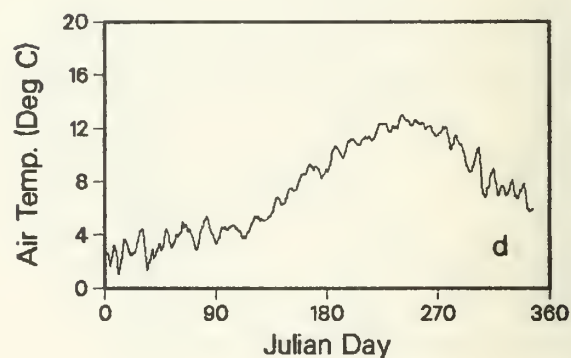
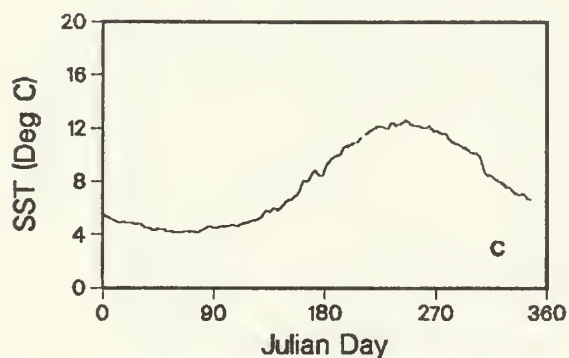
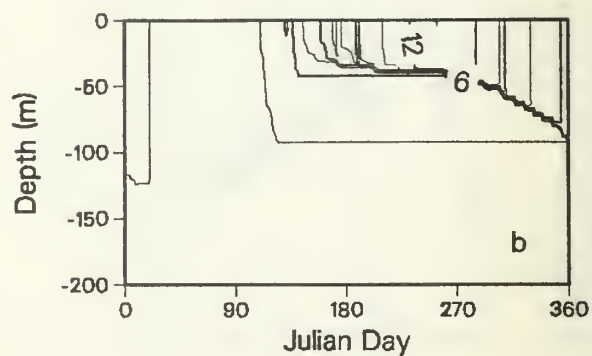
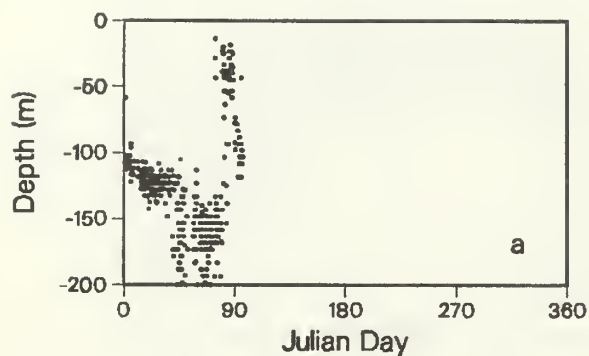


Figure 17. (a) Mixed layer depths from BT drop (b) depth vs. time contours of temperature, (c) sea-surface temperature, (d) air temperature, (e) dew point temperature, (f) wind speed and (g) cloud cover for year 1969.

# INITIAL DISTRIBUTION LIST

1. Defense Technical Information Center 2  
Cameron Station  
Alexandria, Virginia
2. Library, Code 0142 2  
Naval Postgraduate School  
Monterey, California 93940
3. Commanding Officer (Attn: S. Piacsek) 1  
Naval Ocean Research and Developmnt Agency  
NSTL Station, Mississippi 39529
4. Commander 1  
Naval Oceanography Command  
NSTL Station, Mississippi 39529
5. Commanding Officer 1  
Fleet Numerical Oceanography Center  
Monterey, California 93940
6. Officer-in-Charge 1  
Naval Environmental Prediction Research Facility  
Monterey, California 93940
7. Librarian 1  
Naval Environmental Prediction Research Facility  
Monterey, California 93940
8. Commander  
Attn: Code 8100 1  
Attn: Code 6000 1  
Attn: Code 3300 1  
Naval Oceanographic Office  
NSTL Station  
Bay St. Louis, Mississippi 39522
9. Office of Naval Research 1  
Code 481  
NSTL Station, Mississippi 39529
10. Dean of Research, Code 012 1  
Naval Postgraduate School  
Monterey, California 93940
11. Prof. R.L. Elsberry, Code 63Es 1  
Naval Postgraduate School  
Monterey, California 93940
12. Prof. R.W. Garwood, Jr., Code 68Gd 10  
Naval Postgraduate School  
Monterey, California 93940

13.	Department of Meteorology, Code 63Mm Naval Postgraduate School Monterey, California 93940	1
14.	Prof. R.I. Haney, Code 63Hy Naval Postgraduate School Monterey, California 93940	1
15.	Prof. C.N.K. Mooers, Code 68Mr Naval Postgraduate School Monterey, California 93940	1
16.	Prof. R.J. Renard, Code 63Rd Naval Postgraduate School Monterey, California 93940	1
17.	Prof. M. Rienecker, Code 68Rr Naval Postgraduate School Monterey, California 93940	1
18.	Prof. A. Willmott, Code 68Wt Naval Postgraduate School Monterey, California 93940	1
19.	Mr. D. Adamec, Code 63Ac Naval Postgraduate School Monterey, California 93940	5
20.	Mr. P.C. Gallacher, Code 63Ga Naval Postgraduate School Monterey, California 93940	1
21.	Department of Oceanography, Code 68 Naval Postgraduate School Monterey, California 93940	1
22.	Commanding Officer Naval Research Laboratory Attn: Library, Code 2627 Washington, D.C. 20375	1
23.	Naval Research Laboratory Code 2627 Washington, D.C. 20375	1
24.	Office of Naval Research Attn: Code 483 Attn: Code 460 Attn: Code 102E 800 N. Quincy Street Arlington, Virginia 22217	3 1 2

25. Contracting Officer 1  
ONR Code 613C: JMD  
800 N. Quincy Street  
Arlington, Virginia 22217
26. Deputy Under Secretary of Defense 1  
Research and Advanced Technology  
Military Assistant for Environmental Science  
Rccm 3D120  
Washington, D.C. 20301
27. NODC/NOAA 1  
Code D781  
Wisconsin Avenue, N.W.  
Washington, D.C. 20235
28. Commanding Officer 1  
ONR Branch Officer  
Attn: Dr. R.L. Lau  
1030 E. Green Street  
Pasadena, California 91106
29. Dr. David Anderson 1  
DAMTP  
Silver Street  
Cambridge CB3 9EW  
United Kingdom
30. Dr. K. Bryan 1  
GFEL/NOAA  
Princeton University  
P.O. Box 308  
Princeton, New Jersey 08540
31. Dr. Curtis A. Collins 1  
Program Manager  
Environmental Prediction Office of IDOE  
National Science Foundation  
Washington, D.C. 20550
32. Dr. Claude Frankignoul 1  
Dept. of Meteorology, 54-1520  
Massachusetts Institute of Technology  
Cambridge, Massachusetts 02139
33. Dr. Jerry A. Galt 1  
NCAA Pacific Marine Environment Lab.  
University of Washington WB-10  
Seattle, Washington 98105

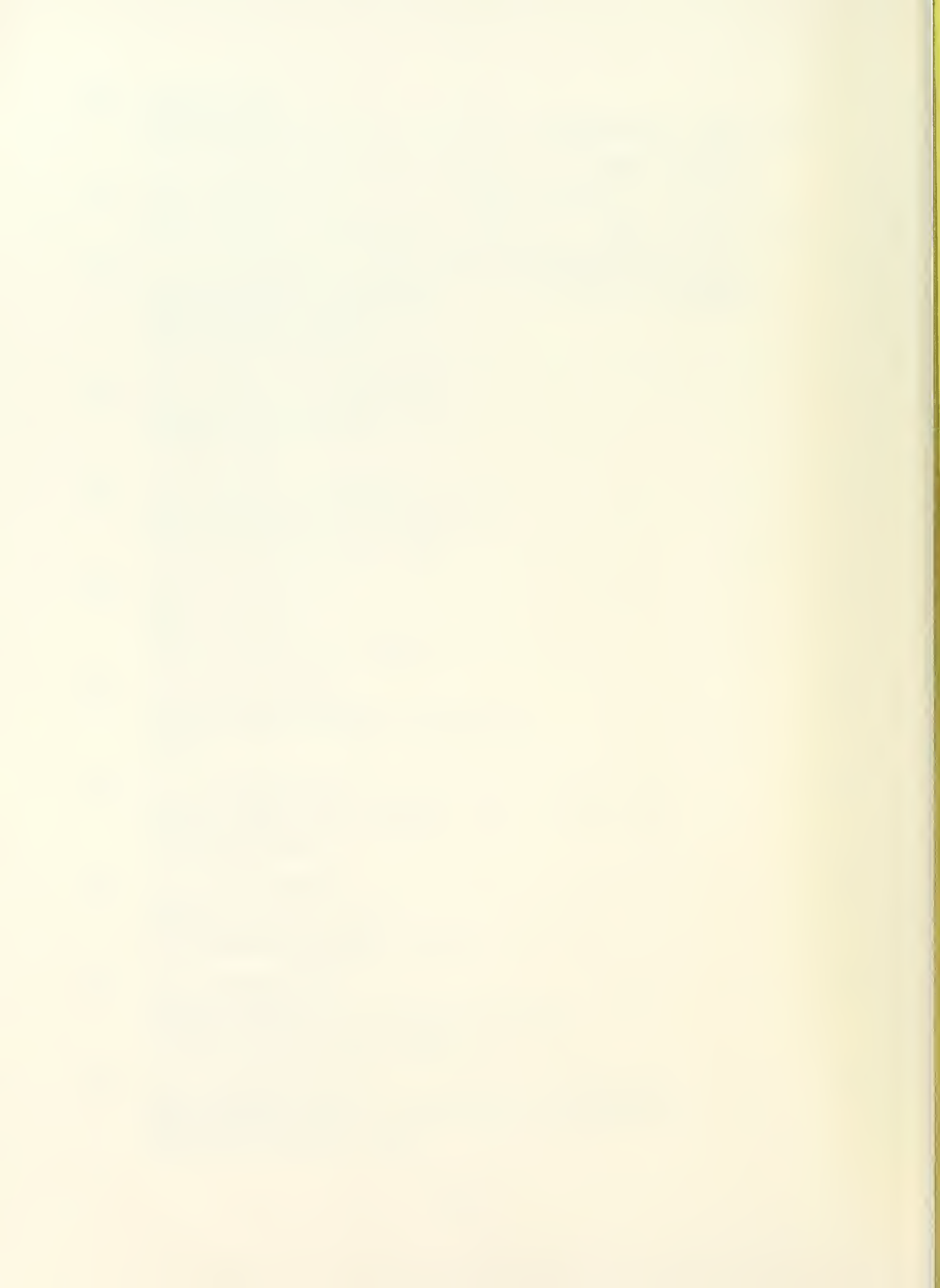
34. Prof. W.L. Gates, Chairman 1  
Dept. of Atmospheric Sciences  
Oregon State University  
Corvallis, Oregon 97331
35. Dr. Adrian Gill 1  
DAMTP  
Silver Street  
Cambridge CB3 9EW  
United Kingdom
36. Dr. Lou Goodman 1  
ONR Code 481  
c/c NUSC, Building 101-N  
Newport, Rhode Island 02840
37. Dr. David Halpern 1  
NCAA/PMEL  
3711 15th Avenue N.E.  
Seattle, Washington 98105
38. Dr. Dale B. Haidvogel 1  
Center for Earth and Planetary Sciences  
Harvard University  
Cambridge, Massachusetts 02138
39. Prof. Y.J. Han 1  
Dept. of Atmospheric Sciences  
Oregon State University  
Corvallis, Oregon 97331
40. Dr. Ed Harrison 1  
Dept. of Earth and Planetary Sciences  
Massachusetts Institute of Technology  
Cambridge, Massachusetts 02139
41. Dr. William Holland 1  
NCAR  
P.O. Box 3000  
Boulder, Colorado 80302
42. Cdr. Robert G. Kirk 1  
ONR Code 481  
NSTL Station, Mississippi 39529
43. Dr. Jeong-Woo Kim 1  
Dept. of Atmospheric Sciences  
Oregon State University  
Corvallis, Oregon 97331
44. Library 1  
Woods Hole Oceanographic Institution  
Woods Hole, Massachusetts 02543



45. Affonso da S. Mascarenhas, Jr. 1  
Dept of Meteorology and Physical Oceanography  
Room 54-1711  
Massachusetts Institute of Technology  
Cambridge, Massachusetts 02139
46. Ekki Mittelstredt 1  
Deutsches Hydrographisches Institut  
Bernhard-Nocht-Strabe 78 Postfach 2 20  
2000 Hamburg 4, F.R.G.
47. Dr. Bob Miller 1  
Harvard University  
Division of Applied Sciences  
Pierce Hall  
Cambridge, Massachusetts 02138
48. Dr. M. Miyake 1  
Institute of Ocean Sciences  
9860 W. Saanich Road  
P.O. Box 5000  
Sidney, B.C. V8L 4B2  
CANADA
49. Dr. Mike McPhaden 1  
NCAR  
P.O. Box 3000  
Boulder, Colorado 80302
50. Dr. J. Namias 1  
Scripps Institution of Oceanography A-030  
LaJolla, California 92093
51. Dr. Peter Niiler 1  
Scripps Institution of Oceanography A-030  
LaJolla, California 92093
52. Dr. J.J. O'Brien 1  
Meteorology Annex  
Florida State University  
Tallahassee, Florida 32306
53. Dr. C. Paul 1  
NOAA/AMOI/PLOL  
15 Rickenbacker Cswy  
Miami, Florida 33149
54. Prof. Allan R. Robinson 1  
Harvard University  
Pierce Hall  
Cambridge, Massachusetts 02138

55. Dr. P. Ripa 1  
CICESE  
P.O. Box 4844  
San Ysidro, California 92073
56. Lcdr. John Roeder 1  
ONR Code 481  
NSTL Station, Mississippi 39529
57. Dr. Tom Sanford 1  
Applied Physics Laboratory  
University of Washington  
1013 NE 40th Street  
Seattle, Washington 98105
58. Prof. Artem S. Sarkisyan 1  
Institute of Oceanol. USSR  
Academy of Sciences  
Moscow, USSR
59. Dr. Robert E. Stevenson 1  
ONR Scientific Liaison Officer  
205 Mathews Campus, UCSD  
LaJolla, California 92093
60. Dr. Bert Semtner 1  
NCAR  
P.O. Box 3000  
Boulder, Colorado 80302
61. Dr. Kenzo Takano 1  
Rikagaku Kenkyusho  
Yamato-Machi, Saitama Prefecture  
JAPAN
62. Dr. Rory Thompson 1  
CSIRO Division of Fisheries and Oceanography  
Box 21, Cronulla, N.S.W.  
AUSTRALIA, 2230
63. Dr. J.D. Thompson 1  
JAYCOR  
205 S. Whiting Street  
Alexandria, Virginia 22304
64. Dr. Warren White 1  
NORPAX A-030  
Scripps Institution of Oceanography  
LaJolla, California 92093
65. Prof. Klaus Wyrtki 1  
University of Hawaii Institute of Geophysics  
2525 Correa Road  
Honolulu, Hawaii 96822

66. Dr. W. Washington 1  
NCAR  
P.O. Box 3000  
Boulder, Colorado 80302
67. Huseyin Yuce 1  
Yuk. Muh. Kd. Yzb.  
Sey. Hid. ve Osl. Da. Bsk. ligi  
Cobuklu/Istanbul  
TURKEY



U205132

DUDLEY KNOX LIBRARY - RESEARCH REPORTS



5 6853 01069546 3

U20513